8-2013

Structural Health Monitoring and Damage Identification of Bridges Using Triaxial Geophones and Time Series Analysis

Reza Vasheghani Farahani
rvashegh@utk.edu

To the Graduate Council:

I am submitting herewith a dissertation written by Reza Vasheghani Farahani entitled "Structural Health Monitoring and Damage Identification of Bridges Using Triaxial Geophones and Time Series Analysis." I have examined the final electronic copy of this dissertation for form and content and recommend that it be accepted in partial fulfillment of the requirements for the degree of Doctor of Philosophy, with a major in Civil Engineering.

Dayakar Penumadu, Major Professor

We have read this dissertation and recommend its acceptance:

Richard M. Bennett, Edwin G. Burdette, Vasileios Maroulas

Accepted for the Council:

Carolyn R. Hodges

Vice Provost and Dean of the Graduate School

(Original signatures are on file with official student records.)

Structural Health Monitoring and Damage Identification of Bridges Using Triaxial Geophones and Time Series Analysis

A Dissertation Presented for the
Doctor of Philosophy
Degree
The University of Tennessee, Knoxville

Reza Vasheghani Farahani
August 2013

To Sarah, Ryan and my parents whom I love more than anything.

Acknowledgements

There are so many people who helped me to accomplish this work that I want to thank them all but one page may not list them all.

First and foremost, I would like to express my deepest and most sincere gratitude to my advisor, Dr. Dayakar Penumadu, for his support and encouragement throughout my Ph.D. work. He has been a reliable and enlightening guide in my research and his mentorship has been critical to the success of this work. I will forever be grateful to him.

I would also like to thank my fabulous dissertation committee members, Dr. Richard M. Bennett, Dr. Edwin G. Burdette, and Dr. Vasileios Maroulas. They have helped me a lot by providing invaluable technical comments which have improved the quality of this research significantly.

Next, I would like to thank all my professors at the University of Tennessee, Knoxville. I would like to extend special thanks to Dr. William S. Ragland and Dr. Richard T. Williams for their help with explanation of the experimental data used in this study. I would also like to thank Dr. Husheng Li, and Ali Taalimi for their technical support and guidance in signal processing and Dr. Wenchao Song for his technical support and guidance in ABAQUS finite element program. I would also like to thank all my friends and peers at the University of Tennessee, Knoxville for their support and encouragement during this research.

To my dear wife Sarah, thank you for your love, support, and encouragement that made it possible for me to accomplish this work.

Abstract

This study uses the vibration data of two full-scale bridges, subjected to controlled damage, along the I-40 west, near downtown Knoxville, TN, to evaluate the feasibility of time series-based damage identification techniques for structural health monitoring. The vibration data was acquired for the entrance ramp to James White Parkway from I-40 westbound, and the I-40 westbound bridge over 4th Avenue, before the bridges were demolished during I-40 expansion project called Smartfix40. The vibration data was recorded using an array of triaxial geophones, highly sensitive sensors to record vibrations, in healthy and damaged conditions of the bridges. The vibration data is evaluated using linear stationary time series models to extract damage sensitive-features (DSFs) which are used to identify the condition of bridge. Two time series-based damage identification techniques are used and developed in this study.

In the first technique, the vibration data is corrected for sensor transfer function suitable for given geophone type and then convolved with random values to create input for autoregressive (AR) time series models. A two-stage prediction model, combined AR and autoregressive with exogenous input (ARX), is employed to obtain DSFs. An outlier analysis method based on DSF values is used to detect the damage. The technique is evaluated using the vertical vibration data of the two bridges subjected to three controlled amounts of known damage on the steel girders.

In the second technique, ARX models and sensor clustering technique is used to obtain prediction errors in healthy and damaged conditions of the bridges. DSF is defined

as the ratio of the standard deviations of the prediction errors. The proposed technique is evaluated using the triaxial vibration data of the two bridges.

This study also presents finite element analysis of the I-40 westbound bridge over 4th Avenue to obtain simulated vibration data for different damage levels and locations. The simulated data are then used in the ARX models and sensor clustering damage identification technique to investigate the effects of damage location and extent, efficacy of each triaxial vibration, and effect of noise on the vibration-based damage identification techniques.

Table of Contents

List of Tables

List of Figures

Chapter 1. Introduction

1.1. Introduction and literature review

The recent collapse of bridges in the U.S. and around the world such as the collapse of the I-35W Bridge in Minneapolis, Minnesota in 2007, Figure 1.1, have raised many concerns regarding the current condition of bridges (Mosavi 2010). In the collapse of the I-35W Bridge which was an eight-lane steel truss bridge, 13 people were killed and 145 people were injured. The bridge failure initiated at gusset plates on the center portion of the deck truss which caused it to have inadequate capacity for the expected loads on the structure (NTSB 2008).

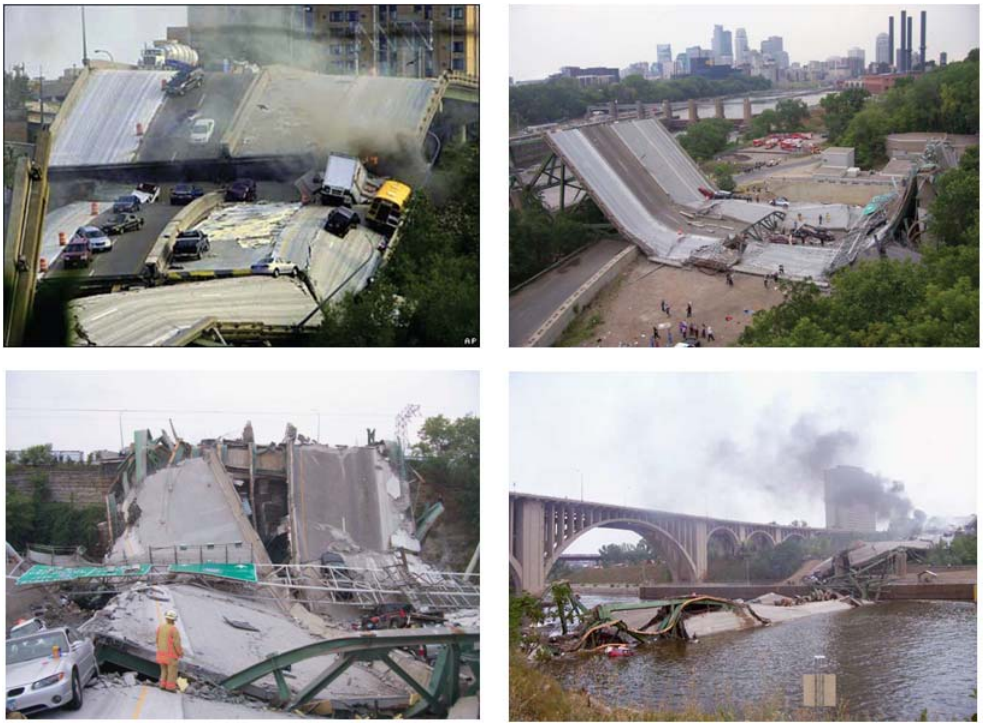

Figure 1.1. I-35W Bridge Collapse, Minneapolis, Minnesota
(Stambaugh and Cohen 2007)

In January 1992, the Holston River Bridge, an eight-span bridge which consisted of four continuous longitudinal girders located in east Knox county, Tennessee, suffered a fatigue failure of the east bound fascia girder. The crack had propagated through the bottom flange of the girder and tore through the web to within a few inches of the top flange as shown in Figure 1.2 (Deatherage et al. 1996). The damage was detected quickly so repairing and retrofitting was begun almost immediately, and no injuries or serious issues were reported.

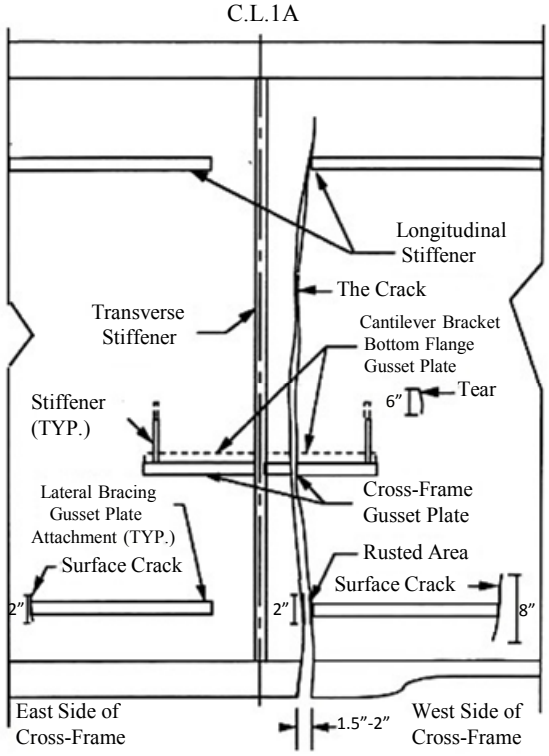

Figure 1.2. Holston River Bridge girder-cracked section (Deatherage et al. 1996)

Currently, bridges in the U.S. are inspected and rated during biennial inspections which rely heavily on visual techniques (Ragland 2011) while such methods for detecting damage are

relatively unreliable (FHWA 2001). As a result, there has been a large amount of effort during the past decade to develop structural health monitoring (SHM) and damage identification techniques.

SHM refers to the observation of a structural system over time and obtaining structural responses using an array of sensors, extraction of damage-sensitive features (DSFs), and statistical analysis to detect changes that may indicate damage in the structure. A common approach for extracting the DSFs from SHM data is to use time series models. When a considered time series model approximates the vibration response of a structure and model coefficients or residual error are obtained, any deviations in these coefficients or residual error can be inferred as an indication of a change or damage in the structure. Depending on the technique employed, various DSFs are proposed to capture the deviations. For example, Sohn and Farrar (2001) presented a two-stage approach implementing combined autoregressive (AR) and autoregressive with exogenous input (ARX) to obtain DSF corresponding to the residual error, the difference between the measured vibration data, and the prediction obtained from the AR-ARX model developed from the healthy condition of the structure. They used an 8 degree-of-freedom mass-spring system and showed that the proposed technique was able to detect and locate the damage. Nair et al. (2006) presented a time series-based damage identification technique within a pattern classification framework. They used autoregressive moving average (ARMA) models and defined the DSF as a function of the first three AR components. They used the analytical and experimental results of an ASCE benchmark structure and indicated that the proposed technique was able to detect and locate the damage. Recently, Gul and Catbas (2011) used ARX models and a sensor clustering technique to detect and locate the damage. They

defined a fit ratio based on the norms of measured output minus predicted output and measured output minus the mean of measured output and used the difference between the fit ratios of the models in healthy and damaged conditions of the structure as a DSF. They applied the technique to a laboratory steel grid structure subjected to different damage scenarios and indicated that damage was detected and located for most of the cases. They also used the data from Z24 bridge (Kramer et al. 1999) where different levels of pier settlement were applied as damage and showed that damage was detected and located with a minimum number of false alarms.

A critical aspect of SHM is data acquisition which involves the source of vibration (ambient loading, drop test,...), the sensor type (unidirectional or triaxial sensors, accelerometer or geophone,...), the sensor's number and location, and the storage and transmittal hardware, whose selections depend on economic considerations (Farrar and Worden 2007). In SHM of bridges, where several sensors are needed, use of unidirectional sensors instead of triaxial sensors can considerably reduce the cost of data acquisition. However, it is important to know the most effective direction of vibration so that the unidirectional sensors can be positioned along that direction. Several researchers have conducted numerical, laboratory and full-scale tests to study the most effective vibrations for SHM (Fasel et al. 2002, Ragland et al. 2011, Cheung et al. 2008). Fasel et al. (2002) simulated a three story building driven by an electro dynamic shaker attached to the base of the structure and reported that sensors in line with the excitation were most effective while the sensors lined up perpendicular to the excitation were quite ineffective. Ragland et al. (2011) presented finite element analysis of a five-girder bridge subjected to vertical vibration source and indicated that horizontal response of the bridge was more sensitive to the damage than the vertical response. Cheung et al. (2008) used the triaxial vibration data of

the Z24 bridge (Kramer et al. 1999) obtained under the ambient loading and reported that similar results were obtained using horizontal and vertical vibration data.

In real-life bridge monitoring, environmental and operational effects, such as changes in temperature (Peeters and Roeck 2001) and noise (Zhang 2007), can make the use of vibration based-damage identification techniques difficult since they can affect the dynamic characteristics of a bridge in a way similar to the damage. Moreover, it has been shown that fundamental frequencies and mode shapes of real-life bridges may not be significantly influenced by local damage (Ragland 2009, Ragland et al. 2011). All of these facts invoke the need for some simplified studies of full-scale bridges to better understand the factors that can affect dynamic characteristics of the bridges and subsequently the ability of vibration-based damage identification techniques to identify the damage.

The main objective of the current study is to develop time series-based damage identification techniques with suitable modifications so that the induced damage in the two full-scale bridges already tested by Ragland (2009) using a drop weight source can be identified. The vibration data considered is unique, as it was obtained for full-scale bridges in undamaged states and after known amounts of damage had been induced in the steel girders. The two types of bridges chosen in the study represent about 70% of existing bridges in the state of Tennessee in terms of their spans, connectivity, and structural details; thus, a successful study will potentially have a large impact. Another objective of the current study is to present a sensitivity study using simulated vibration data obtained from finite element analysis to investigate the effects of damage location and extent, efficacy of each triaxial vibration, and effect of noise on vibration-based damage identification techniques.

1.2. References

Cheung, A., Cabrera, C., Sarabandi, P., Nair, K.K., Kiremidjian, A. and Wenzel, H. (2008). "The application of statistical pattern recognition methods for damage detection to field data." *Smart Mater. Struct.*, 17 (6), 065023.

Deatherage, J. H., Goodpasture, D. W., Clarke, S. N., Burdette, E. G. (1996). "Fatigue evaluation of the Holston River Bridge." *Final Report No.* TN-RES1028.

Farrar, C.R. and Worden, K. (2007). "An introduction to structural health monitoring." *Phil. Trans. R. Soc. A*, 365, 303-315.

Fasel, T.R., Gregg, S.W. , Johnson, T.J., Farrar, C.R. and Sohn, H. (2002). "Experimental modal analysis and damage detection in a simulated three story building." *Proc. 20th IMAC Conference on Structural Dynamics*, Los Angeles, CA.

Federal Highway Administration (FHWA) (2001). "Reliability of visual inspection for highway bridges." *Report No.* FHWA-RD-01–020, Washington, D.C.

Gul, M. and Catbas, F.N., (2011). "Damage assessment with ambient vibration data using a novel time series analysis methodology" *J. Struct. Eng.*, 137(12), 1518-1526.

Kramer, C., De Smet, C. A. M., and De Roeck, G. (1999). "Z24 bridge damage detection tests." *Proc.17th Int. Modal Analysis Conf. (IMAC XXVII)*, Society for Experimental Mechanics (SEM), Bethel, CT, 1023–1029.

Mosavi, A.A. (2010). "Vibration-based damage detection and health monitoring of bridges" Ph.D. Dissertation, North Carolina State University, NC.

Nair, K. K., Kiremidjian, A. S., and Kincho, H. L. (2006). "Time series-based damage detection and localization algorithm with application to the ASCE benchmark structure." *J. Sound Vib.*, 291 (1–2), 349–368.

National Transportation Safety Board (NTSB) (2008). "Collapse of I-35W Highway Bridge, Minneapolis, Minnesota, August 1, 2007."*Accident Report No*. NTSB/HAR-08/03.

Peeters, B. and Roeck, GD. (2001). "One-year monitoring of the Z24-Bridge: environmental effects versus damage events." *Earthquake Eng Struct Dyn,* 30(2), 149–71.

Ragland, W. S. (2009). "Structural health monitoring and damage evaluation of full-scale bridges using triaxial geophones: controlled in-situ experiments and finite element modeling." Ph.D. Dissertation, Dept. of Civil and Environmental Engineering, University of Tennessee, Knoxville, TN.

Ragland, W. S., Penumadu, D. and Williams, R. T. (2011). "Finite element modeling of a full-scale five-girder bridge for structural health monitoring." *Struct. Health Monit.*, 10(5), 449-465.

Sohn, H. and Farrar, C.R. (2001). "Damage diagnosis using time series analysis of vibration signals." *Smart Mater. Struct.*, 10(3), 446- 451.

Stambaugh, H. and Cohen, H. (2007). "I-35W bridge collapse and response Minneapolis, Minnesota August 1, 2007." Dept. of Homeland Security, U.S. Fire Administration.

Zhang, Q.W. (2007). "Statistical damage identification for bridges using ambient vibration data." Comput. Struct., 85(7-8), 476-485.

Chapter 2. Full-scale bridge damage identification using time series analysis of a dense array of geophones excited by drop weight

Reza Vasheghani-Farahani and Dayakar Penumadu

My primary contributions to this chapter included: (1) gathering and reviewing literature, (2) processing and analyzing all the vertical data, (3) filter designing, (4) writing and developing MATLAB codes for implementing time-series based damage identification technique, (5) adapting an outlier analysis method to detect the damage (6) developing the idea of using convolution with random values to create suitable input required for Autoregressive (AR) models, and (7) most of the writing.

2.1. Abstract

This study presents an innovative technique for damage identification of full-scale bridge structures on I-40 through downtown Knoxville, Tennessee excited by a drop weight. The dynamic data, obtained using a dense array of geophones which are highly sensitive to record vibrations, is evaluated using time series analysis. The directly measured vibration data is convolved with random values to create suitable input for time series analysis of two full-scale highway bridges that were subjected to known amounts of damage to the bridge girder at chosen locations. A two-stage prediction model, combined autoregressive (AR) and autoregressive with exogenous input (ARX), is employed to obtain damage-sensitive features. An outlier analysis method is used to detect the damage. The proposed technique is evaluated using the vertical vibration data of the two full-scale bridges subjected to three controlled levels of known damage on the steel girders. The results of the analysis performed on the 126 data sets indicate that the proposed technique is able to detect the damage even when damage level is small and damage is located near a support. However, the proposed technique cannot consistently identify the location of damage.

2.2. Introduction

The recent collapse of bridges in the U.S. and around the world such as the collapse of the I-35W Bridge in Minneapolis, Minnesota in 2007 has significantly increased the awareness about bridge safety and the renewed need for reliable structural health monitoring techniques (Mosavi 2010). Currently, bridges in the U.S. are inspected and rated every two years based on visual techniques (Ragland 2011) which are useful for identifying visible damage in areas clearly accessible, but

are relatively unreliable for identifying fatigue or crack-based damage (Ragland et al. 2011, FHWA 2001) and are also very labor intensive.

In recent years, Structural Health Monitoring (SHM) of bridges has received increasing attention for implementing a damage detection strategy. It consists of observation of a bridge system over time using an array of sensors and obtaining structural responses, extraction of damage-sensitive features from structural responses, and statistical analysis to detect changes that may indicate damage in the bridge. A common approach for extracting the damage-sensitive features (DSFs) from SHM data to identify the damage is to use time series models. When a considered time series model approximates the vibration response of a structure and model coefficients and residual error are obtained, any deviations in these coefficients or residual error can be inferred as an indication of a change or damage in the structure. Depending on the technique employed, various damage-sensitive features are proposed to capture the deviations. For example, Sohn and Farrar (2001) presented a two-stage approach implementing combined autoregressive (AR) and autoregressive with exogenous input (ARX). They used the residual error, the difference between the measured vibration data and the prediction obtained from the AR-ARX model developed from the healthy condition of the structure, as damage-sensitive feature. Nair et al. (2006) presented a time series-based damage identification technique within a pattern classification framework. They used autoregressive moving average (ARMA) models and defined the damage-sensitive features as a function of the first three AR components. Recently, Gul and Catbas (2011a) used ARX models and sensor clustering damage identification method to detect and locate the damage. They defined a fit ratio based on the norms of measured output minus predicted output and measured output minus mean of measured output and used the

difference between the fit ratios of the models in healthy and damaged conditions of the structure as a damage-sensitive feature.

The autoregressive (AR) models used in time series-based damage identification techniques require that the input to the system is white noise. This requirement is usually satisfied in either of two ways: (1) ambient vibrations are recorded (Conte et al. 2008; Farrar et al. 1994; Farrar et al. 2000; Kramer et al. 1999), and (2) a shaker is used to apply the white noise loading (Mosavi et al. 2012; Sohn and Farrar 2001). The present study extends and evaluates such approach for using vibration response to a deterministic excitation source, such as a simple and repeatable drop weight source, to evaluate the occurrence and spatial location of damage in bridge structures. It uses a technique based on the convolution of vibration response of sensors with white noise to simulate the response from the white noise excitation source. An averaging technique is then used to minimize the effect of added randomness on the final results. The proposed technique is applied to two full-scale damaged bridges tested by our research group in the recent past (Ragland 2009) using a drop source. The objective of the current study is to develop AR-ARX damage identification technique with suitable modifications so that the induced damage in the two full-scale bridges that were studied can form a basis for generalization of this simple and inexpensive structural health monitoring technique without the need for permanent instrumentation. The vibration data considered is unique, as it was obtained from full-scale bridges before and after inducing known amounts of damage to the steel girders. The two types of bridges chosen in this study are very common in the state of Tennessee in terms of spans, connectivity, and structural details; thus a successful study is expected to have a large impact.

2.3. Damage identification procedure

2.3.1. Geophone sensors and transfer function

A geophone is a passive velocity sensor which is inexpensive, highly sensitive for detecting very small amplitudes of vibrations, developed for oil industry and vibration monitoring market. It typically comprises of a magnetic mass moving within a wire coil surrounded by a casing as shown in Figure 2.1. Relative movement of the magnetic mass to the wire coil, resulting from a given vibration source, induces a voltage that can be converted to the velocity.

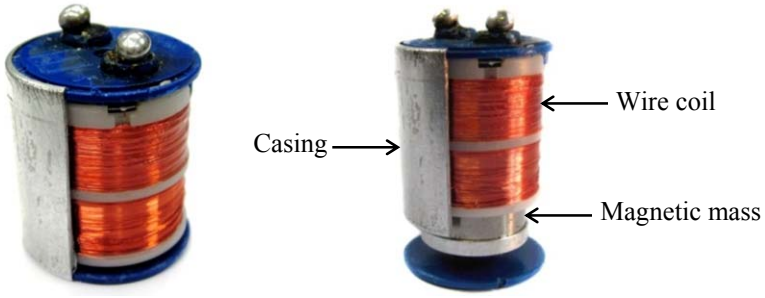

Figure 2.1. A typical Mark Products LRS-1000 geophone

Geophones are more beneficial than accelerometers for structural health monitoring applications that involves large number of sensors and small amplitude dynamic data because their unit cost is usually less, and they do not need any additional amplification or conditioning (Ragland et al. 2010, 2011). However, the output of a geophone needs to be corrected for magnitude and phase shifts due to the nature of their frequency response function. The output of a geophone sharply reduces linearly below its natural frequency, 9.984 Hz for this study, and thus requires adjustments based on its transfer function. Furthermore, when the frequency content of the signal is around the natural frequency, the geophone output induces known

amount of phase shift which can also be readily corrected using the transfer function of a given geophone. To correct the geophone's output (voltage) for the magnitude and phase shifts the following transfer function shown in Eq. (2.1) is used.

$$\frac{\mathrm{V}}{\dot{\mathrm{X}}} = \frac{-G\left(\frac{\omega}{\omega_n}\right)^2}{\left[1-\left(\frac{\omega}{\omega_n}\right)^2\right] + 2i\zeta\frac{\omega}{\omega_n}} \tag{2.1}$$

where V is the geophone output (voltage), $\dot{\mathrm{X}}$ is the corrected geophone output (velocity), ω_n is the natural frequency of the geophone, ζ is the damping ratio of the geophone, i is the imaginary unit such that $i^2 = -1$, ω is the excitation frequency and G is the sensitivity of the geophone.

2.3.2. Linear stationary time series model

A time series is a sequence of observations of a variable over time. A linear stationary time series model representing the input-output relationship maybe written as shown in Eq. (2.2) (Ljung 1999)

$$v(t) + a_1 v(t-1) + \cdots + a_{n_a} v(t-n_a) = b_1 u(t-1) + \cdots + b_{n_b} u(t-n_b) + e(t) + c_1 e(t-1) + \cdots + c_{n_c} e(t-n_c) \tag{2.2}$$

where, *v(t)* is output at time *t*, $v(t-1) \ldots v(t-n_a)$ are previous outputs on which the current output depends, $u(t-1) \ldots u(t-n_b)$ are previous inputs on which the current output depends, and *e(t)* is white noise. $n_a, n_b,$ and n_c are the model orders and a_i, b_i and c_i are model unknown

parameters. This difference equation can be written in a compact form as shown in Eq. (2.3) which is often referred in the literature as autoregressive moving average model with exogenous input (ARMAX).

$$A(q)v(t) = B(q)u(t) + C(q)e(t) \tag{2.3}$$

where q^{-1} is the backward shift operator and *A(q)*, *B(q)* and *C(q)* are polynomials represented in Eq. 2.4a to 2.4c.

$$A(q) = 1 + a_1 q^{-1} + \cdots + a_{n_a} q^{-n_a} \tag{2.4a}$$

$$B(q) = b_1 q^{-1} + \cdots + b_{n_b} q^{-n_b} \tag{2.4b}$$

$$C(q) = 1 + c_1 q^{-1} + \cdots + c_{n_c} q^{-n_c} \tag{2.4c}$$

When $n_c = 0$, the ARMAX model simplifies to the ARX model shown in Eq. (2.5). Similarly, when $n_b = n_c = 0$, the ARMAX model simplifies to the AR model shown in Eq. (2.6). The present study uses these two time series models, shown in Eqs. (2.5) and (2.6), for identifying the induced damage in the two full-scale bridges.

$$v(t) + a_1 v(t-1) + \cdots + a_{n_a} v(t-n_a) = b_1 u(t-1) + \cdots + b_{n_b} u(t-n_b) + e(t) \tag{2.5}$$

$$v(t) + a_1 v(t-1) + \cdots + a_{n_a} v(t-n_a) = e(t) \tag{2.6}$$

2.3.3. Drop weight excitation source and autoregressive models

The autoregressive (AR) models require that the input to the system is white noise (Brockwell and Davis 1991) while the vibration data used in this study corresponds to response of bridges to a controlled drop weight source which is not a white noise type excitation; therefore, drop weight

vibration response cannot be used directly in AR models. To simulate the dynamic response of the bridges for white noise excitation; a new idea is implemented based on the convolution approach (Williams 2012).

Convolution is used in linear systems to obtain the response of a system under any excitation if the impulse response of the system is known (Sadiku 1987). In general, the convolution of two signals *x(t)* and *h(t)* is represented by the symbol '*' and defined by Eq. (2.7):

$$y(t) = x(t) * h(t) = \int_{-\infty}^{+\infty} x(\tau)h(t-\tau)d\tau \tag{2.7}$$

where τ is a dummy variable and *y(t)* is the convolution of *x(t)* and *h(t)*. In order to obtain the response of a bridge for white noise input from drop test response, *x(t)* is defined as normally distributed random values with a mean of zero and unit standard deviation representing the white noise and *h(t)* is selected as the drop test response. This convolution technique is illustrated in Figure 2.2 for a typical drop weight source response employed in our research.

In Figure 2.2(a), a typical drop test response of a bridge with a length of 4 seconds is shown. This response is convolved with white noise with a length of 4 seconds, shown in Figure 2.2(b), to obtain the anticipated response of the system under the white noise input as shown in Figure 2.2(c). As can be seen, the convolved response will have a decay part which starts after the original response length and corresponds to unloading. Since the response of the bridge under the white noise loading is required in this study, this decaying part is disregarded. Figure 2.3 summarizes the steps required to create random data from the drop weight source response recorded by an array of sensors (geophones) to use in AR models.

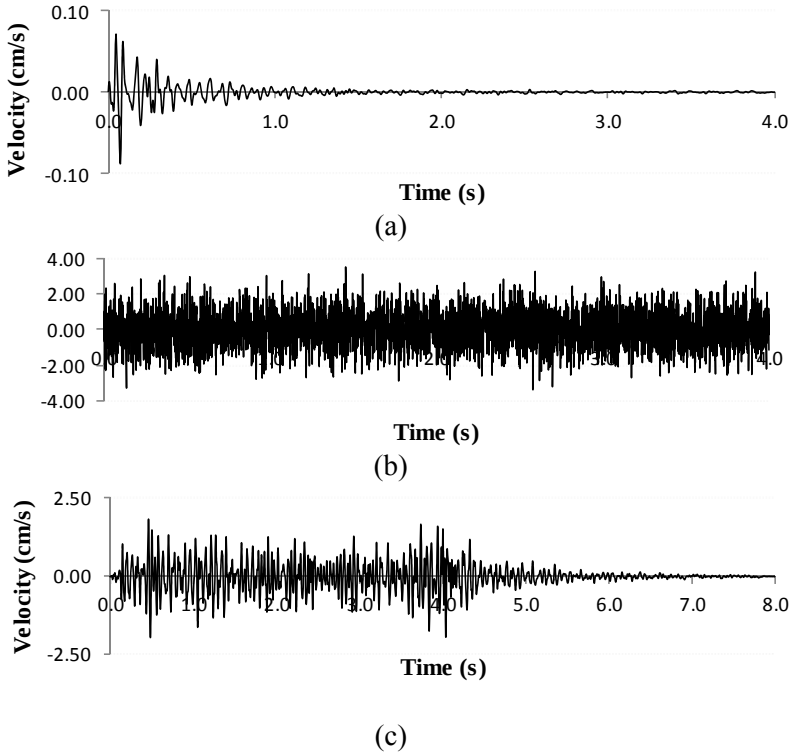

Figure 2.2. Convolution of a drop test response with white noise: (a) A typical drop test response (b) White noise (c) The drop test response convolved with the white noise

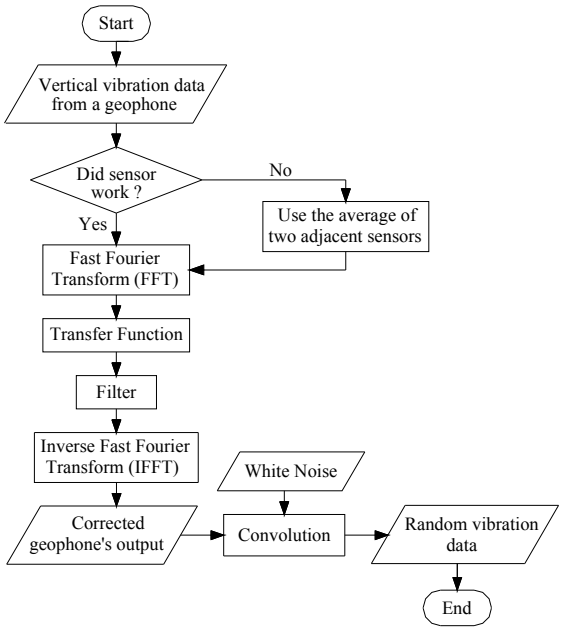

Figure 2.3. Creating random data from drop test response recorded by a geophone

After obtaining the vibration data for white noise input and before applying any autoregressive model, this data is normalized according to Eq. (2.8) to be comparable at a sensor location.

$$v_i(t) = \frac{\hat{v}_i(t) - \mu_i}{\sigma_i} \tag{2.8}$$

where $\hat{v}_i$ is the convolved velocity of geophone i and v_i is the normalized convolved velocity of geophone i. μ_i and σ_i are mean and standard deviation of the convolved velocity of geophone i, respectively.

2.3.4. Creating databases and selecting the reference signal

For damage identification in which unknown signals are compared with the signals obtained during the healthy condition of a structure, it is important to create databases from the signals obtained in healthy condition of the structure under different ambient conditions so that the unknown signals can be compared with the reference signals obtained in similar ambient condition. Sohn and Farrar (2001) presented a methodology to find the most similar signal from the database based on the Euclidean distance. First, all the signals in a database and the unknown (damaged) signal are approximated with an autoregressive (AR) model with an order of n_a as shown in Eq. (2.9) and Eq. (2.10) for undamaged and damaged cases, respectively.

$$v_u(t) + a_1 v_u(t-1) + \cdots + a_{n_a} v_u(t-n_a) = e_u(t) \tag{2.9}$$

$$v_d(t) + b_1 v_d(t-1) + \cdots + b_{n_a} v_d(t-n_a) = e_d(t) \tag{2.10}$$

where the subscripts of *u* and *d* denote the undamaged and damaged conditions, respectively. Then, from several signals in the database, the signal that minimizes the difference of AR coefficients shown in Eq. (2.11) is selected as the reference signal for that unknown signal.

$$Difference = \sum_{i=1}^{n_a} (a_i - b_i)^2 \tag{2.11}$$

2.3.5. Damage-sensitive feature selection

A two-stage prediction model combining an AR model and an ARX model (Sohn and Farrar 2001) is used to compute the damage-sensitive features. In the first stage, at each sensor location, a reference signal is calculated and suitable model order of AR, n_a, is determined. Then AR models with the order of n_a, AR(n_a), is constructed for the healthy and damaged conditions as shown in Eq. (2.12) and Eq. (2.13), respectively.

$$v_u(t) + a_1 v_u(t-1) + \cdots + a_{n_a} v_u(t-n_a) = e_{u,1}(t) \tag{2.12}$$

$$v_d(t) + b_1 v_d(t-1) + \cdots + b_{n_a} v_d(t-n_a) = e_{d,1}(t) \tag{2.13}$$

The second subscript of 1 denotes the first stage of the prediction model. For the construction of a two-stage prediction model, it is assumed that the error between the measurement and the prediction obtained in healthy case, $e_{u,1}(t)$, is mainly caused by unknown external input; therefore, an ARX model can be defined. ARX model with the orders of n_b and n_c are constructed in healthy condition as shown in Eq. (2.14).

$$v_u(t) + c_1 v_u(t-1) + \cdots + c_{n_b} v_u(t-n_b) = d_1 e_{u,1}(t-1) + \cdots + d_{n_c} e_{u,1}(t-n_c) + e_{u,2}(t) \tag{2.14}$$

where the second subscript of 2 denotes the second stage of the prediction model. The ARX model obtained in healthy condition is used for the damaged condition to investigate the relationship of $e_{d,1}(t)$ and $v_d(t)$:

$$v_d(t) + c_1 v_d(t-1) + \cdots + c_{n_b} v_d(t-n_b) = d_1 e_{d,1}(t-1) + \cdots + d_{n_c} e_{d,1}(t-n_c) + e_{d,2}(t) \qquad (2.15)$$

If the model obtained from the healthy condition is not a good representation of the unknown signal, there would be a significant change in the standard deviation of the residual error. Therefore, the standard deviation ratio of the residual errors, $\sigma(e_{d,2})/\sigma(e_{u,2})$, is used as damage-sensitive feature to identify the existence and spatial location of the damage.

2.3.6. Identification of the damage occurrence

This study uses an outlier analysis method to identify the damage occurrence corresponding to the observed values falling above a threshold value by adapting a methodology similar to Worden et al. (2000) where a Monte Carlo method was used. First, random data are created for healthy condition of the structure by convolving the data obtained in healthy condition of the structure with white noise for various geophone sensors; corresponding to various spatial locations on the bridge and damage-sensitive features (DSFs) are calculated. The process is repeated many times and DSFs are saved (in this study, the process is repeated and 5,000 DSFs are saved). The DSFs are sorted and the value above which only 5% of the simulations occur is selected as the threshold value, below which the bridge structure can be considered healthy. Physical states corresponding to observed data falling above the threshold (outlier) can be considered as damaged states.

2.4. Full-Scale I-40 bridge data sets used for the analysis

This study uses the data of two full-scale damaged bridges along the I-40 west downtown Knoxville, to evaluate the proposed approach for damage identification. The test data was acquired for two bridges corresponding to the entrance ramp to James White Parkway from I-40 westbound, and the I-40 westbound bridge over 4th Avenue, before the bridges were demolished during I-40 expansion project called Smartfix40 (Ragland 2009). The test bridges corresponded to: (1) a three-girder bridge in which damage was located at the mid-span of an exterior girder (case 1), and (2) a five-girder bridge in which damage was located near a support on an interior girder (case 2). Information about these two bridges and related data acquisition aspects are briefly explained here.

2.4.1. Case 1: A three-girder bridge damaged at mid-span

The entrance ramp to James White Parkway from I-40 westbound was constructed in 1967 in Knoxville, TN. It was a 30° skewed bridge consisting of three spans supported by three steel girders as shown in Figures 2.4 and 2.5.

Figure 2.4. Photo of the entrance ramp to James White Parkway from I-40 westbound

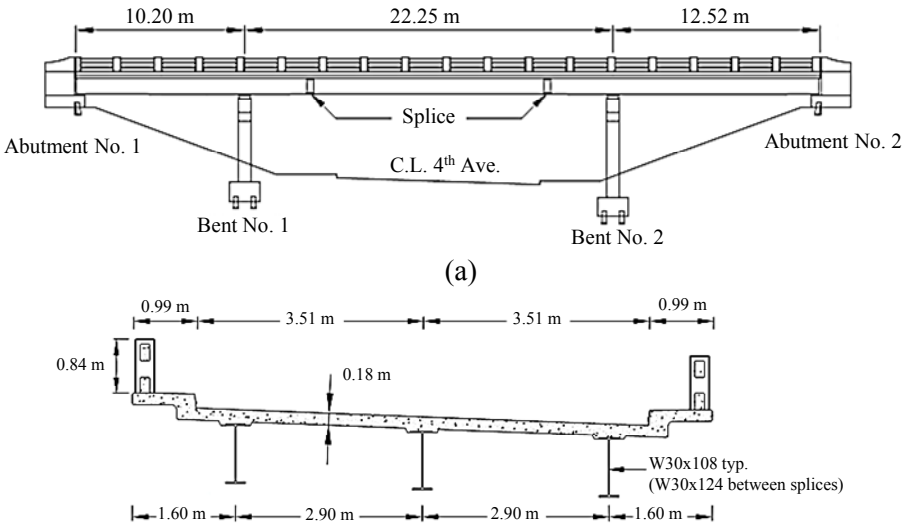

Figure 2.5. Entrance ramp to James White Parkway from I-40 westbound (a) Longitudinal profile (b) Cross-section (modified from Ragland 2009)

This bridge was instrumented with geophones made by Mark Products (LRS-1000) to measure the vertical vibrations. Figure 2.6 shows an example array of geophones installed on the bridge deck to measure the vibrations corresponding to locations along the center beam. Sensor parameters corresponding to natural frequency, damping ratio, and sensitivity of these vertical geophones were experimentally determined as 9.984 Hz, 0.6076 and 160.6 mV/(cm/s) to use in field data correction procedure using the transfer function described earlier. The bridge was excited by a drop source, a 22.7 kg sandbag, dropped from a height of one meter on the bridge deck at six locations shown in Figure 2.7 and the vibration data were recorded.

Figure 2.6. An array of Geophones installed on the bridge deck over the center beam

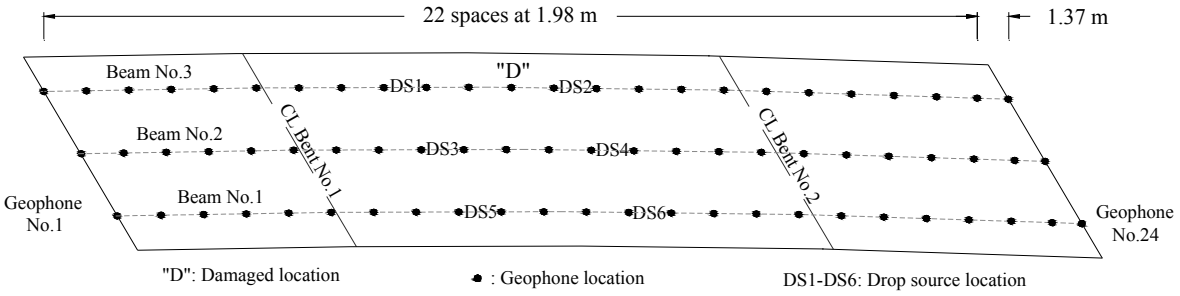

Figure 2.7. Plan view of the entrance ramp to James White Parkway

Vibration data was recorded at a total of 72 geophone locations shown in Figure 2.7, with a sampling rate of 1000 Hz for a total of 4 seconds using a 48-channel seismograph. The 72 measurement locations were divided into three groups along the beam lines and drop test was repeated for each beam line until all 72 measurements were covered. Three damage scenarios shown in Figure 2.8, were applied to the beam No. 3 at mid-span of the bridge's center span by incrementally cutting the beam upward from the bottom flange.

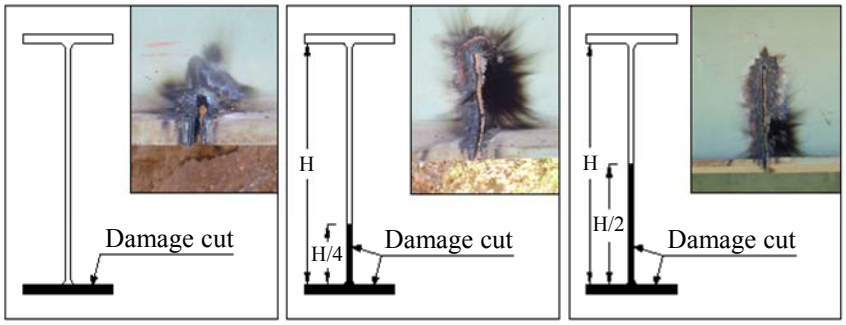

Figure 2.8. Induced damage scenarios: (a) Bottom flange cut (D1) (b) Bottom flange plus ¼ of the web cut (D2) (c) Bottom flange plus ½ the web cut (D3)

The proposed technique is applied to the measured vertical data sets using a MATLAB code after correcting the data considering the sensor transfer function. A sine-squared tapered band-pass filter with the corner frequencies of 2, 3, 55 and 60 Hz is used for the corrections. These corner frequencies are selected based on the fact that the resolution of geophones degrades at low frequencies and also the electrical noise frequency is largely 60 Hz in the U.S. All the signals are convolved with normally distributed random values with a mean of zero and unit standard deviation to simulate the bridge tests for white noise input. The convolved data are then normalized. A database is created from the signals obtained in healthy condition of the bridge for every sensor location. To find a suitable reference signal for comparing corresponding output for damaged state at each sensor location, an AR model with the order of 20 is implemented in this study to obtain the most similar signal from the database based on Eq. (2.11). At each sensor location, the suitable AR model order is determined using the reference signal. A maximum AR model order of 20 is set for the analysis based on the Akaike Information Criterion (AIC) (Ljung 1999) and the suitable model order is determined using the Minimum Description Length (MDL) criterion (MATLAB 2011). When AR model order is determined at each sensor location, AR

models are created for all the signals in healthy and damaged conditions to find the residual errors. These residual errors are used as input to ARX models. The reference signals and their residual errors obtained from the AR models are used to find the suitable ARX model orders (n_b and n_c) at each sensor location. In order to determine the suitable ARX model orders, the maximum model orders are limited to 3 to prevent any overfeeding. The reference data are split to two parts, where the first part is used for the estimation and the second part is used for the validation. The best model is then selected by comparing the output of the models with orders ranging from 1 to 3 with the validation data set. When the appropriate model orders are determined, ARX models are constructed for all the signals in healthy condition to find the residual errors. For each sensor, the same ARX model obtained in healthy condition of the bridge is used for the damaged condition to obtain the residual error in damaged condition. Damage-sensitive feature (DSFs) is computed as the ratio of the standard deviation of the residual error in damaged condition to the standard ratio of the residual error in healthy condition. Since the proposed technique is based on the convolution with random values and potentially the choice of randomness could affect the predictions, this process is repeated several times and the average of DSFs at each sensor location is identified as illustrated in Figure 2.9 for data set No. 4 when the drop source was located as DS1.

As shown in Figure 2.9, the implemented technique has successfully detected outliers for damage scenarios D2 and D3 while no outlier is detected for damage scenario D1 which indicate that damage is just detected for damage scenarios D2 and D3. For both cases that the existence of damage is successfully identified, it is seen that the maximum outliers are found at locations

other than the induced damage location; therefore, damage is not located. The procedure is repeated for the other vertical vibration data sets and all the results are summarized in Table 2.1.

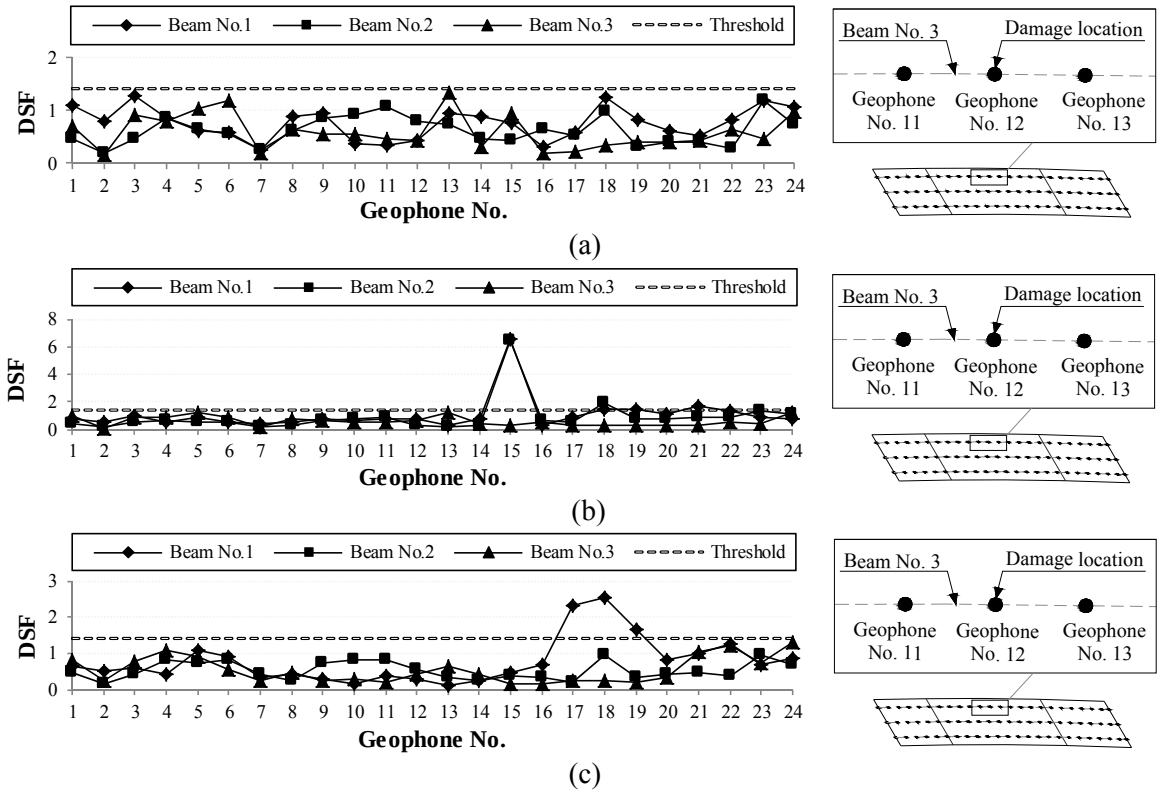

Figure 2.9. Damage identification results of the entrance ramp to James White Parkway for the data set No. 4 when drop source was located as DS1 (a) Damage scenario D1 (b) Damage scenario D2 (c) Damage scenario D3

As shown in Table 2.1, for all the damage scenarios, the approach implemented in this study using the vertical vibration data sets is able to identify the occurrence of damage with minimum false decision. It is seen that from 72 cases studied here, damage is not correctly detected for just 1 case which corresponds to small damage level.

While the used two-step prediction technique had already shown to be able to locate the damage in simple laboratory model (Sohn and Farrar 2001), the results of the analysis presented in Table 2.1 indicate that it cannot consistently locate the damage in a real-life structure. It is seen that from 72 vertical vibration data sets used in this study, just in 7 cases damage is spatially located and only in 19 cases the damaged beam is correctly identified. Failure in locating the damage in this real-life bridge can be related to the high degree of redundancy of the bridge, uncertainties in repeated tests and measurements, and different ambient conditions which all can affect the damage identification results.

Table 2.1. Summary of damage identification results for the entrance ramp to James White Parkway

Drop Source Location	Data Set No.	Damage scenario		
		D1	D2	D3
DS1	1	●	□	□
	2	□	□	□
	3	□	□	□
	4	---	□	□
DS2	1	□	□	○
	2	□	□	○
	3	□	□	□
	4	○	□	□
DS3	1	●	●	●
	2	○	□	●
	3	●	□	●
	4	○	□	□
DS4	1	○	□	□
	2	○	□	□
	3	□	□	□
	4	○	□	○
DS5	1	○	□	□
	2	□	□	□
	3	□	□	□
	4	□	□	○
DS6	1	□	□	□
	2	□	□	□
	3	□	□	□
	4	○	□	□

●Damage spatially located; ○ Damage located on the damaged beam.
□ Damage detected but not located; --- Damage not detected.

It seems from Table 2.1 that damage localization results are improved when drop source is located on the middle girder causing the whole structure to vibrate. However, no success is found in locating the damage when drop source is located near the bent No. 2 shown in Figure 2.7. The bridge drawings show that the girder-bent connections at the bent No. 2 resist the girders rotation around the bent axis causing the vibration of the bridge to be limited when drop source is located near the bent No. 2. Therefore, it seems that optimized results are obtained when the whole structure is vibrated and the vibration amplitudes are maximized.

2.4.2. Case 2: A five-girder bridge damaged near a support

The I-40 westbound bridge over 4th Avenue is used for evaluating the feasibility of damage identification proposed here when damage is located near a support for a highly structurally redundant bridge with very high chance of re-distribution of external loads. The considered bridge was a 45° skewed bridge consisting of three spans supported by five steel girders as shown in Figures 2.10 and 2.11.

Figure 2.10. Photo of the I-40 westbound bridge over 4th Avenue

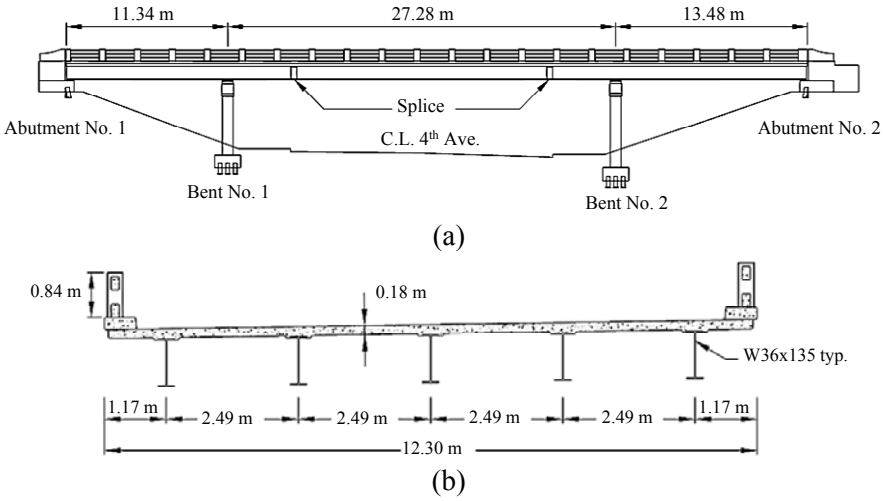

Figure 2.11. I-40 westbound bridge over 4th Avenue: (a) Longitudinal profile (b) Cross-section (modified from Ragland 2011)

The bridge was excited by dropping the sandbag from a height of one meter on the bridge deck at nine locations shown in Figure 2.12. Data was recorded at a total of 120 measurement locations with a sampling rate of 1000 Hz for a total of 3 seconds using the 48-channel seismograph. The 120 measurement locations were divided into five groups along the beam lines to obtain the vibration measurements. The same damage scenarios mentioned earlier for case 1 were implemented for this bridge as well. Damage was located on an interior girder close to a support to further study the effectiveness of damage identification techniques for cases where damage is near a support as it is expected that vibration-based damage detection is less reliable at locating the damage occurring near a support (Zhou et al. 2007).

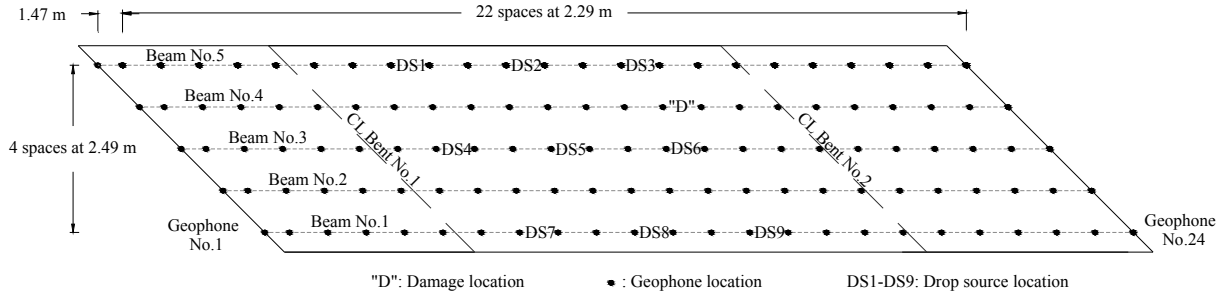

Figure 2.12. I-40 westbound bridge over 4th Avenue: geophone layout (modified from Ragland et al. 2011)

The same damage identification procedure mentioned earlier for case 1 is repeated here to identify the induced damage on the I-40 westbound bridge over 4th Avenue. Table 2.2 summarizes the results of the damage identification for all the vertical vibration data sets recorded during the test.

As shown in Table 2.2, the proposed technique has successfully detected the induced damage located on an interior girder near a support for all the studied cases, even when the induced damage is small. However, just in two cases spatial location of the damage has been successfully identified which indicate that the proposed vibration-based damage identification technique cannot successfully locate the damage occurred near a support. It is also seen that from 54 vertical vibration data sets studied, just in 15 cases damaged beam is correctly identified. Therefore, it is clear that the implemented damage identification technique cannot successfully identify the damaged beam too. Compared with case 1, it is seen that when damage is located on an interior girder near a support, the chance of spatially locating the damage considerably decreases.

Table 2.2. Summary of damage identification results for the I-40 westbound bridge over 4th Avenue

Drop Source Location	Data Set No.	Damage scenario		
		D1	D2	D3
DS1	1	□	○	□
	2	□	□	□
DS2	1	○	□	○
	2	○	□	□
DS3	1	□	□	□
	2	□	○	□
DS4	1	□	□	□
	2	□	□	□
DS5	1	□	□	□
	2	●	□	●
DS6	1	□	□	□
	2	□	○	○
DS7	1	□	□	□
	2	○	□	□
DS8	1	○	□	□
	2	□	□	□
DS9	1	○	○	○
	2	□	○	□

●Damage spatially located; ○ Damage located on the damaged beam.
□ Damage detected but not located; --- Damage not detected.

2.5. Conclusions

This study presents an innovative technique for damage identification of bridge structures using a controlled drop weight source, inexpensive array of geophones, and time series analysis. The vibration data recorded by an array of geophones is corrected for magnitude and phase shifts and then convolved with white noise to create suitable input required for autoregressive time series models. A two-stage prediction model, combined autoregressive (AR) and autoregressive with exogenous input (ARX), is employed to calculate damage-sensitive feature which is defined as the ratio of the standard deviation of residual error in damaged condition to the standard deviation of residual error in healthy condition. An outlier analysis method is used to identify the

existence of damage. The proposed technique is verified using the vertical vibration data sets of two full-scale bridges subjected to controlled levels of known damage on the steel girders.

- The damage detection results using the vibration data sets of the two test bridges indicate that the proposed damage identification technique is able to identify the existence of damage, even when damage level is small and damage is located at an obscure position such as near a support on an interior girder.

- The damage localization results on the two full-scale bridges with three and five steel girders indicate that the proposed damage identification technique cannot consistently locate the damage. It is seen that when damage is located on an interior girder near a support, the chance of locating the damage using the implemented damage identification technique considerably reduces.

- It is also seen from the analysis results of the three-girder bridge damaged at mid-span of an exterior girder that damage localization results are improved when the vibration source is located in a place that the whole structure vibrates and the vibration amplitudes are maximized.

2.6. Acknowledgments

The authors would like to acknowledge Drs. William S. Ragland, Richard T. Williams, Vasileios Maroulas, Husheng Li, and Mongi A. Abidi and Ali Taalimi at the University of Tennessee, Knoxville for their technical support and guidance.

2.7. References

Brockwell, P.J. and Davis, R.A. (1991). *Time Series: Theory and Methods*, second ed., Springer-Verlag, NY.

Conte, J.P., He, X.F., Moaveni, B., Masri, S.F., Caffrey, J.P., Wahbeh, M., Tasbihgoo, F., Whang, D.H., and Elgamal, A. (2008). "Dynamic testing of Alfred Zampa Memorial Bridge." *J. Struct. Eng.*, 134(6), 1006-1015.

Farrar, C.R., Baker, W.E., Bell, T.M., Cone, K.M., Darling, T.W., Duffey, T.A., Eklund, A., and Migliori, A. (1994). "Dynamic characterization and damage detection in the I-40 Bridge over the Rio Grande." *Report No.* LA-12767-MS, Los Alamos National Laboratory, Los Alamos, NM.

Farrar, C.R., Cornwell, P.J., Doebling, S. W., and Prime, M.B. (2000). "Structural health monitoring studies of the Alamosa Canyon and I-40 bridges." *Report No.* LA-13635-MS, Los Alamos National Laboratory, Los Alamos, NM.

Federal Highway Administration (FHWA) (2001). "Reliability of visual inspection for highway bridges." *Report No.* FHWA-RD-01–020, Washington, D.C.

Gul, M. and Catbas, F.N., (2011a) "Damage assessment with ambient vibration data using a novel time series analysis methodology" *J. Struct. Eng.*, 137(12), 1518-1526.

Gul, M. and Catbas, F. N. (2011b) "Structural health monitoring and damage assessment using a novel time series analysis methodology with sensor clustering." *J. Sound Vib.*, 330(6), 1196-1210.

Kramer, C., De Smet, C. A. M., and De Roeck, G. (1999). "Z24 bridge damage detection tests." *Proc.,17th Int. Modal Analysis Conf. (IMAC XXVII)*, Society for Experimental Mechanics (SEM), Bethel, CT, 1023–1029.

Ljung, L. (1999). *System identification: theory for the user*, second ed., Prentice-Hall, Upper Saddle River, NJ.

MATLAB version 7.12 [Computer software]. (2011). The MathWorks Inc., Natick, MA.

Mosavi, A.A. (2010). "Vibration-based damage detection and health monitoring of bridges" Ph.D. Dissertation, North Carolina State University, NC.

Mosavi, A.A., Dickey, D., Seracino, R. and Rizkalla, S. (2012). "Identifying damage locations under ambient vibrations utilizing values autoregressive models and Mahalanobis distances." *Mech. Syst. Signal Process.*, 26, 254–267.

Nair, K. K., Kiremidjian, A. S., and Kincho, H. L. (2006). "Time series-based damage detection and localization algorithm with application to the ASCE benchmark structure." *J. Sound Vib.*, 291 (1–2), 349–368.

Ragland, W. S. (2009). "Structural health monitoring and damage evaluation of full-scale bridges using triaxial geophones: controlled in-situ experiments and finite element modeling." Ph.D. Dissertation, Dept. of Civil and Environmental Engineering, University of Tennessee, Knoxville, TN.

Ragland, W. S., Penumadu, D. and Williams, R. T. (2010). "Using geophones for nondestructive evaluation of full-scale bridges", *Transp. Res. Rec.*, Transportation Research Board, No. 2201, 45–52.

Ragland, W. S., Penumadu, D. and Williams, R. T. (2011). "Finite element modeling of a full-scale five-girder bridge for structural health monitoring." *Struct. Health Monit.*, 10(5), 449-465.

Sadiku, M.N.O (1987) "Convolution with singularity functions", *IEEE Transactions on education*, E30 (1), 52-54

Sohn, H. and Farrar, C.R. (2001). "Damage diagnosis using time series analysis of vibration signals." *Smart Mater. Struct.*, 10(3), 446- 451.

Williams, R.T. (2012). Personal communication, University of Tennessee, Knoxville, TN, April

Worden, K., Manson, G., and Fieller, N. J. (2000). "Damage detection using outlier analysis." *J. Sound Vib.*, 229 (3), 647-667.

Zhou, Z, Wegner, L. D. and Sparling, B. F. (2007). "Vibration-based detection of small-scale damage on a bridge deck." *J. Struct. Eng.*, 133(9), 1257–1267.

Chapter 3: Triaxial damage identification of full-scale bridges excited by drop weight using time series analysis

Reza Vasheghani-Farahani and Dayakar Penumadu

My primary contributions to this chapter included: (1) gathering and reviewing literature, (2) processing and analyzing of all field data, (3) filter designing, (4) writing and developing MATLAB codes for implementing time-series based damage identification technique, (5) adapting an outlier analysis method to detect the damage (6) developing the idea of using convolution with random values (7) defining a new damage-sensitive feature, and (8) most of the writing.

3.1. Abstract

This study presents a new technique for damage identification of bridges using a drop weight and time series analysis. In this technique, the bridge is excited by dropping the drop weight on the bridge deck and vibration data is recorded using a dense array of geophones, highly sensitive sensors. The vibration data is corrected with regard to the geophones properties and then convolved with random values to create vibration data under random loading. Autoregressive with exogenous input (ARX) models and sensor clustering technique is used to obtain prediction errors in healthy and damaged conditions of the bridge. Damage-sensitive features are defined as the ratio of the standard deviations of the prediction errors to identify the existence and location of damage. The proposed technique is verified using the triaxial vibration data of two full-scale bridges in Knoxville, Tennessee subjected to controlled level of damage to the bridge girder. The damage identification technique is performed independently for each triaxial vibration to investigate the efficacy of each vibration in detecting and locating the induced damage. The results of the analysis indicate that the proposed damage identification technique can detect the damage in real-life bridges, even when damage is located near a support on an interior girder. The triaxial analysis results indicate that for the two test bridges excited mainly vertically, all the triaxial vibration data are able to detect the damage; however, none of them can consistently identify the spatial location of the damage.

3.2. Introduction

In recent years, Structural Health Monitoring (SHM) of bridges has received increasing attention for implementing a damage detection strategy. It consists of observation of the bridge over time

and obtaining structural responses using an array of sensors, extraction of damage-sensitive features (DSFs), and statistical analysis to detect changes that may indicate damage in the structure. A common approach for extracting the DSFs from SHM data to identify the damage is using time series models. When a time series model approximates the vibration response of a structure and model coefficients or residual error are obtained, any deviations in these coefficients or residual error can be inferred as an indication of a change or damage in the structure. Several time series-based damage identification algorithms have been proposed and developed by different researchers to extract the DSFs which can identify the damage (Gul and Catbas 2011a,b, Lu and Gao 2005, Nair et al. 2006, Omenzetter and Brownjohn 2006, Sohn and Farrar 2001). Sohn and Farrar (2001) presented a two-stage prediction model, combined autoregressive (AR) and autoregressive with exogenous input (ARX), to obtain DSF corresponding to the residual error, the difference between the measured vibration data and the prediction obtained from the AR-ARX model developed from the healthy condition of the structure. Lu and Gao (2005) presented a new damage identification method based on linear dynamic equations and formulated in the form of ARX time series model. They defined DSF as the standard deviation of the residual error which was the difference between the measured signal and the predicted signal from the ARX model created from a reference state. Nair et al. (2006) presented a time series-based damage identification technique within a pattern classification framework. They used autoregressive moving average (ARMA) models and defined DSF as a function of the first three AR components. Recently, Gul and Catbas (2011a,b) presented a new damage identification technique based on ARX models and sensor clustering to

identify damage. They defined DSF based on the norms of measured output minus predicted output and measured output minus mean of measured output.

A critical aspect of SHM is data acquisition which involves the source of vibration (ambient loading, drop test,...), the sensor type (unidirectional or triaxial sensors, accelerometer or geophone,...), the sensors number and location, and the storage and transmittal hardware, whose selections depend on the economic consideration (Farrar and Worden 2007). In SHM of bridges, where several sensors are needed, use of unidirectional sensors instead of triaxial sensors can considerably reduce the cost of data acquisition. However, it is important to know the most effective direction of vibration so that the unidirectional sensors can be lined up in that direction. Several researchers have conducted numerical, laboratory and full-scale tests to study the most effective vibrations for SHM (Fasel et al. 2002, Ragland et al. 2011, Cheung et al. 2008). Fasel et al. (2002) simulated a three story building driven by an electro dynamic shaker attached to the base of the structure and reported that sensors in line with the excitation were most effective while the sensors lined up perpendicular to the excitation were wholly ineffective. Ragland et al. (2011) presented finite element analysis of a five-girder bridge subjected to vertical vibration source and indicated that horizontal response of the bridge was more sensitive to the damage than the vertical response. Cheung et al. (2008) used the triaxial vibration data of the Z24 bridge (Kramer et al. 1999) obtained under the ambient loading and reported that similar results were obtained using horizontal and vertical vibration data.

The objective of the current study is first developing the ARX model and sensor clustering damage identification technique with suitable modifications so that the induced damage in the two full-scale bridges tested by Ragland (2009) can be identified. These two

bridges represent about 70% of existing bridges in the state of Tennessee considering their span, connectivity and structural detail; thus, successful study is expected to have a large impact. Second, by applying the technique in three global directions, the efficacy of each triaxial vibration on SHM of the bridges is investigated. Several data sets are studied so that a generalized conclusion can be made for this simple and inexpensive SHM technique.

3.3. Damage identification procedure

3.3.1. An introduction to geophones

A geophone is a passive velocity sensor which is inexpensive, highly sensitive to small vibrations, developed for oil industry and vibration monitoring market. It typically comprises of a magnetic mass moving within a wire coil surrounded by a casing as shown in Figure 3.1. Relative movement of the magnetic mass to the wire coil, resulting from a given vibration source, induces a voltage that can be converted to the velocity.

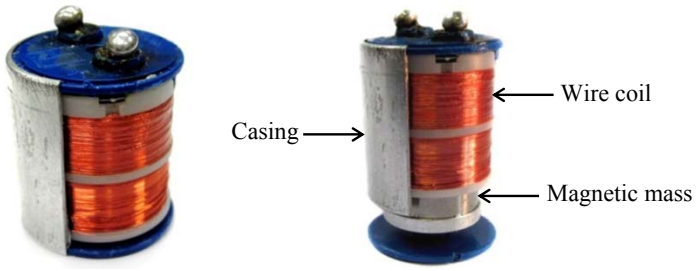

Figure 3.1. A typical Mark Products LRS-1000 geophone

Geophones are more beneficial than accelerometers for structural health monitoring applications that involve large number of sensors and small amplitude dynamic data because

their unit cost is usually less, and they do not need any additional amplification or conditioning (Ragland et al. 2010, 2011). However, the output of a geophone needs to be corrected for magnitude and phase shifts due to the nature of its frequency response function. The output of a geophone sharply reduces linearly below its natural frequency and thus requires adjustments based on its transfer function. Furthermore, when the frequency content of a signal is around the natural frequency of the geophone, the geophone output induces known amount of phase shift which can also be readily corrected using the transfer function of a given geophone. To correct the geophone's output (voltage) for the magnitude and phase shifts the transfer function shown in Eq. (3.1) is used.

$$\frac{\mathrm{V}}{\dot{\mathrm{X}}} = \frac{-G\left(\frac{\omega}{\omega_n}\right)^2}{\left[1-\left(\frac{\omega}{\omega_n}\right)^2\right] + 2i\zeta\frac{\omega}{\omega_n}} \tag{3.1}$$

where V is the geophone output (voltage), $\dot{\mathrm{X}}$ is the corrected geophone output (velocity), ω_n is the natural frequency of the geophone, ζ is the damping ratio of the geophone, i is the imaginary unit such that $i^2 = -1$, ω is the excitation frequency and G is the sensitivity of the geophone.

3.3.2. An introduction to ARX time series models

A linear stationary time series model representing the input-output relationship can be written as shown in Eq. (3.2), which is known as the autoregressive moving average model with exogenous input (ARMAX) (Ljung 1999).

$$A(q)v(t) = B(q)u(t) + C(q)e(t) \tag{3.2}$$

where $v(t)$ is output at time t, $u(t)$ is input at time t, and $e(t)$ is white noise. $A(q)$, $B(q)$ and $C(q)$ are polynomials shown in Eq. 3.3a to 3.3c.

$$A(q) = 1 + a_1 q^{-1} + \cdots + a_{n_a} q^{-n_a} \tag{3.3a}$$

$$B(q) = b_1 q^{-1} + \cdots + b_{n_b} q^{-n_b} \tag{3.3b}$$

$$C(q) = 1 + c_1 q^{-1} + \cdots + c_{n_c} q^{-n_c} \tag{3.3c}$$

where q^{-1} is the backward shift operator, n_a, n_b, and n_c are model orders and a_i, b_i and c_i are model unknown parameters. When $n_c = 0$, the ARMAX model simplifies to the ARX model shown in Eq. (3.4). The structure of this ARX model is shown in Figure 3.2.

$$A(q)v(t) = B(q)u(t) + e(t) \tag{3.4}$$

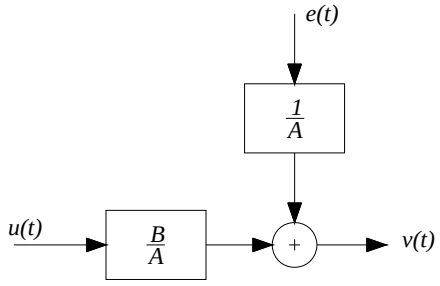

Figure 3.2. The ARX model structure (adapted from Ljung 1999)

3.3.3. ARX models and sensor clustering damage identification technique

In ARX models and sensor clustering damage identification technique (Gul and Catbas 2011a,b), several sensor clusters are defined and ARX models are created for each cluster in healthy

condition of the structure. These models are then employed for the data obtained in damaged condition of the structure to estimate DSFs. In this study, this technique is applied to vibration data obtained from drop weight test and convolved with random values with a mean of zero and unit standard deviation. For all sensors, the convolved data are first normalized according to Eq. (3.5) to be comparable at a sensor location:

$$v_i(t) = \frac{\hat{v}_i(t) - \mu_i}{\sigma_i} \tag{3.5}$$

where $\hat{v}_i$ is the convolved velocity of geophone i and v_i is the normalized convolved velocity of geophone i. μ_i and σ_i are mean and standard deviation of the convolved velocity of geophone i, respectively. After normalizing the convolved vibration data, several sensor clusters are defined and ARX models shown in Eq. (3.6) are created for each cluster in healthy condition of the structure.

$$A(q)v_r(t) = B(q)v(t) + e(t) \tag{3.6}$$

where $v_r(t)$ is the convolved velocity response at the reference sensor (geophone) of a cluster, and $v(t)$ is the matrix of the convolved velocity responses of the sensors inside the cluster.

To explain the methodology, a bridge girder with 24 sensors is illustrated in Figure 3.3. As shown, for a girder with 24 sensors, 24 clusters are defined having one reference sensor each. The first cluster includes two sensors, the reference sensor and the sensor next to it. For the second cluster, there are three sensors in which the middle one is considered as the reference sensor. Clusters 3-23 are defined similarly to the second cluster. The last cluster is defined similarly to the first cluster where the reference sensor is the last sensor. For each of these

clusters, the inputs to the ARX models are the convolved outputs of the sensors in the cluster, while the ARX model output is the convolved output of the reference sensor.

After creating the ARX models in healthy condition of the structure, these models are used for the convolved data obtained from damaged condition to estimate the prediction errors. A new damage-sensitive feature is defined as the ratio of the standard deviation of the prediction error in damaged condition to the standard deviation of the prediction error in healthy condition.

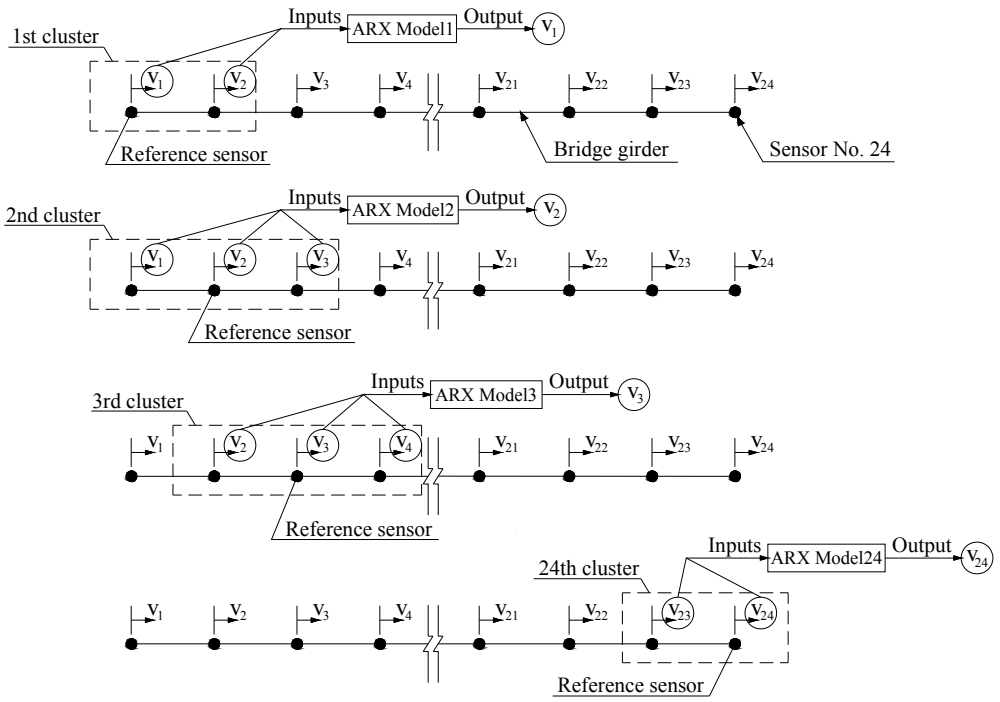

Figure 3.3. Creating ARX models for different sensor clusters along a bridge girder with 24 sensors

To detect the damage, an outlier analysis method is used. A methodology similar to Worden et al. (2000) where a Monte Carlo method was used is adapted. A threshold is defined by using a numerical simulation technique where 5000 simulations are conducted. For each

simulation, the data obtained in healthy condition of the structure is convolved with random values with a mean of zero and unit standard deviation and DSF is calculated and saved. The DSFs are sorted and the value above which only 5% of the simulations occur is selected as the threshold value, below which the structure can be considered as healthy.

3.4. Full-Scale I-40 bridge test data

This study uses the data of two full-scale damaged bridges along the I-40 west downtown Knoxville, to evaluate the proposed damage identification technique. The test data was acquired for the entrance ramp to James White Parkway from I-40 westbound, and the I-40 westbound bridge over 4th Avenue, before the bridges were demolished during I-40 expansion project called Smartfix40 (Ragland 2009). The test bridges corresponded to: (1) a three-girder bridge in which damage was located at the mid-span of an exterior girder (case 1), and (2) a five-girder bridge in which damage was located near a support on an interior girder (case 2). Information about these two bridges and related data acquisition aspect are briefly explained here. More information about the experimental tests can be found in Ragland (2009).

3.4.1. Case 1: A three-girder bridge damaged at mid-span

3.4.1.1. Description of the bridge and data acquisition

The entrance ramp to James White Parkway from I-40 westbound was constructed in 1967 in Knoxville, TN. It was a 30° skewed bridge consisting of three spans supported by three steel girders as shown in Figures 3.4 and 3.5.

Figure 3.4. Photo of the entrance ramp to James White Parkway from I-40 westbound

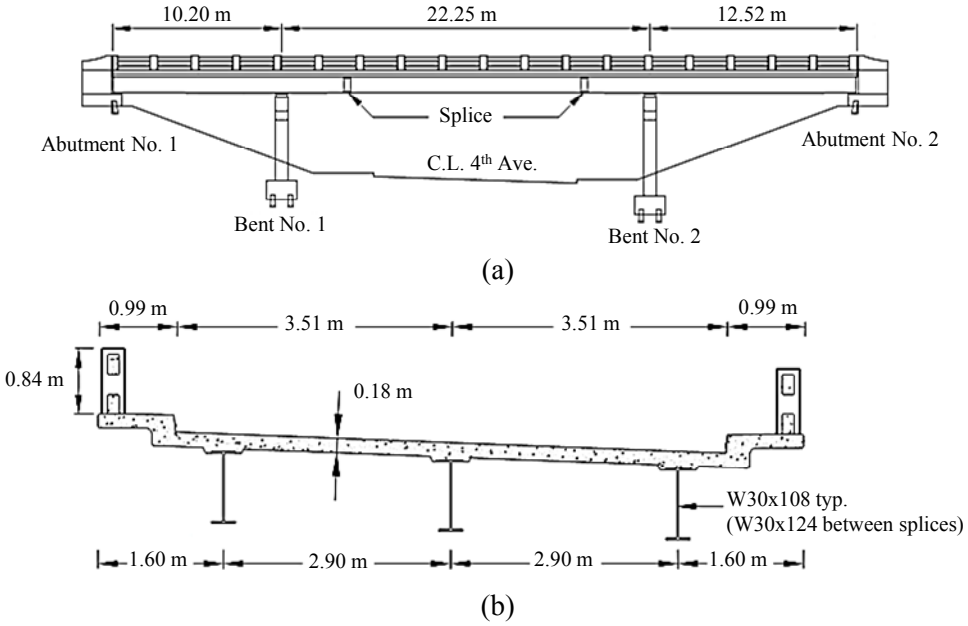

Figure 3.5. Entrance ramp to James White Parkway from I-40 westbound (a) Longitudinal profile (b) Cross-section (modified from Ragland 2009)

This bridge was instrumented with triaxial geophones to obtain vibration measurements. Inexpensive geophones, Mark Products LRS-1000 and Mark Products L-28LBH were used as vertical and horizontal geophones, respectively. Table 3.1 presents the geophones parameters determined experimentally.

Table 3.1. Experimentally determined geophone parameters

Parameter	Geophone Type	
	LRS-1000	L-28LBH
Frequency, ω_n (Hz)	9.984	5.070
Damping Ratio, ζ	0.6076	0.4252
Sensitivity (mV/(cm/s))	160.6	348.0

The bridge was excited vertically by a drop source, a 22.7 kg sandbag, dropped from a height of one meter at six locations, shown in Figure 3.6, on the bridge deck and vibration data was recorded in three global directions.

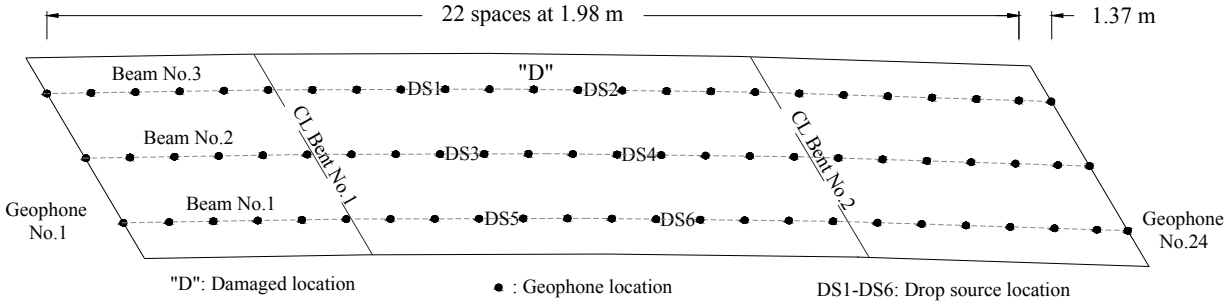

Figure 3.6. Plan view of the entrance ramp to James White Parkway from I-40 westbound

Vibration data was recorded at a total of 72 geophone locations shown in Figure 3.6, with a sampling rate of 1000 Hz for a total of 4 seconds using a 48-channel seismograph. The 72 measurement locations were divided into three groups along the beam lines. For each group of sensors, the sandbag was dropped and the vertical and transverse vibration data were recorded; then, the transverse sensors were rotated by 90° and the sandbag was dropped again to obtain the vertical and longitudinal vibration data. Once the data was recorded for all the three directions,

the line of sensors was shifted to the next beam line and the tests were repeated until all the 72 measurement locations were covered.

Progressive damage scenarios were induced on the beam No. 3 at mid-span of the bridge's center span by cutting the bottom flange towards the half of the web height to simulate a crack that may occur due to fatigue or excessive vehicle weight (Ragland 2009). In this study, the vibration data corresponding to the bottom flange plus half of the web height cut is used for the analysis.

3.4.1.2. Data analysis and results

The triaxial vibration data already obtained by dropping a 22.7 kg sandbag at six locations shown in Figure 3.6, is used in the proposed damage identification technique. The vibration data recorded by the geophones are corrected for magnitude and phase shifts using Eq. (3.1) and a sine-squared tapered band-pass filter with the corner frequencies of 2, 3, 55 and 60 Hz is applied. These corner frequencies are selected based on the fact that the resolution of geophones degrades at low frequencies and also the electrical noise frequency is largely 60 Hz in the U.S. The corrected vibration data is first convolved with random values with a mean of zero and unit standard deviation to simulate the response of the bridge for random loading. 24 sensor clusters are defined along each beam line and ARX models are created for each cluster in healthy condition of the bridge. In order to determine the suitable ARX model orders, first maximum model orders are set to 5 to prevent any overfeeding. Then the convolved data obtained from healthy condition of the structure is split to two parts, where the first part is used for the estimation and the second part is used for the validation. The best model is then selected by

comparing the output of the models with orders ranging between 1 and 5 with the validating data (Matlab 2011). The ARX models determined in healthy condition of the bridge are used for the data obtained in damaged condition and convolved with random values to find the prediction errors and to calculate the damage-sensitive features. Since the proposed technique is based on the convolution with random values and potentially the choice of randomness could affect the predictions, this process is repeated several times and the average of DSFs at each sensor location is identified as illustrated in Figure 3.7 for the vertical data set of 1 when drop source was located at DS1.

As shown in Figure 3.7, the implemented technique has successfully detected outliers which indicate that damage is detected. The maximum DSF is found at geophone No. 13 on the beam No. 3 where the damage was induced during the test. Therefore, spatial location of the damage is correctly identified. The procedure is repeated for other vibration data sets and all the results are summarized in Table 3.1. Here, longitudinal direction refers to the bridge length direction whereas transverse refers to the direction perpendicular to the bridge length.

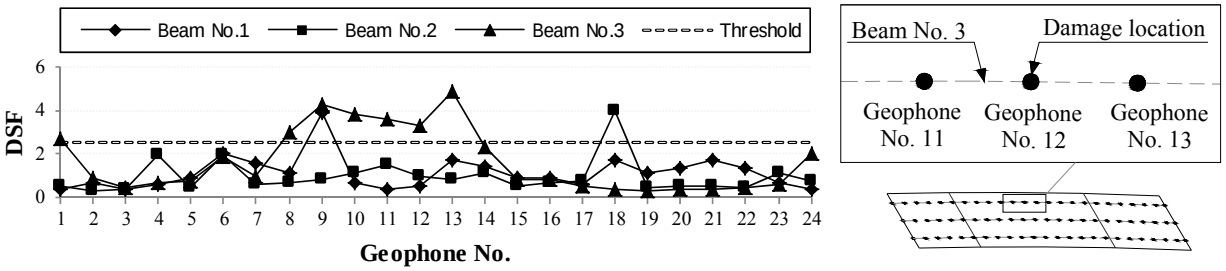

Figure 3.7. Results of the damage identification for the entrance ramp to James White Parkway using the first vertical data set when drop source was located at DS1

Table 3.2. Damage identification results summary for the entrance ramp to James White Parkway

Drop Source Location	Data Set No.	Vibration Component		
		Longitudinal	Transverse	Vertical
DS1	1	N/A	□	●
	2	N/A	□	□
	3	○	N/A	□
	4	○	N/A	□
DS2	1	N/A	□	○
	2	N/A	□	□
	3	□	N/A	○
	4	□	N/A	□
DS3	1	N/A	□	●
	2	N/A	□	●
	3	○	N/A	●
	4	○	N/A	□
DS4	1	N/A	□	□
	2	N/A	○	□
	3	□	N/A	□
	4	○	N/A	○
DS5	1	N/A	□	□
	2	N/A	□	□
	3	○	N/A	○
	4	○	N/A	○
DS6	1	N/A	□	□
	2	N/A	○	□
	3	○	N/A	○
	4	○	N/A	○

●Damage spatially located; ○ Damage located on the damaged beam;
□ Damage detected but not located; --- Damage not detected; N/A data is not available

As shown in Table 3.2, the implemented damage identification technique is able to detect the induced damage in the entrance ramp to James White Parkway. It is seen that all the triaxial vibration data can be used to identify the existence of damage when bridge is damaged at mid-span of an exterior girder and vibrated mainly vertically.

From Table 3.2, it is clear that none of the triaxial vibrations can consistently locate the damage using the implemented damage identification technique. Side by side comparison of the vibrations recorded simultaneously reveals that vertical vibrations are better choices to locate the damage than the horizontal vibrations when the main excitation source is vertical. It is seen that

from 24 vertical vibration data sets, damage has been spatially located for 4 cases while none of the horizontal vibration data sets could locate the damage. Therefore, it seems that vibration along the dominant excitation source is the best option to line up the unidirectional sensors for SHM applications.

3.4.2. Case 2: A five-girder bridge damaged near a support

3.4.2.1. Description of the bridge and data acquisition

The I-40 westbound bridge over 4th Avenue is used for evaluating the feasibility of damage identification proposed here when damage is located near a support for a highly structurally redundant bridge with very high chance of re-distribution of external loads. The considered bridge was a 45° skewed bridge consisting of three spans supported by five steel girders as shown in Figures 3.8 and 3.9.

Figure 3.8. Photo of the I-40 westbound bridge over 4th Avenue

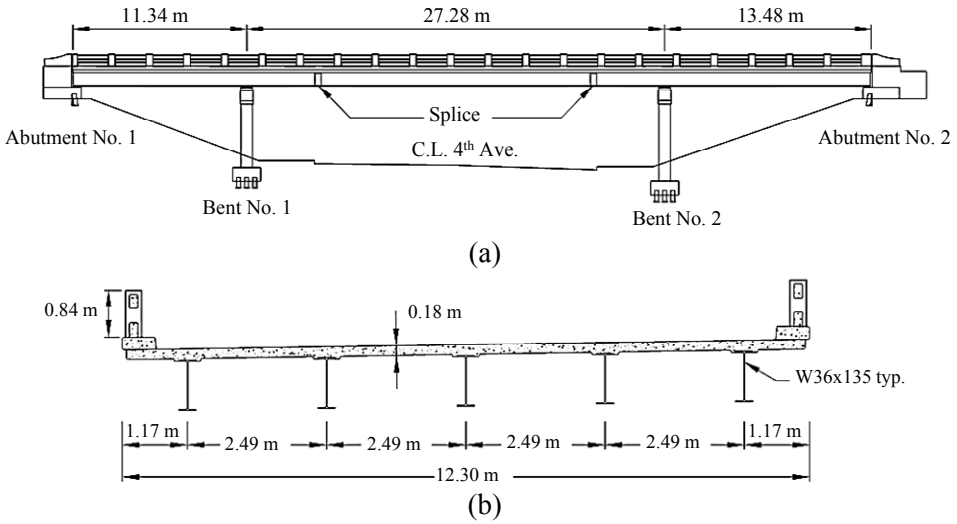

Figure 3.9. I-40 westbound bridge over 4th Avenue: (a) Longitudinal profile (b) Cross-section (modified from Ragland et al. 2011)

This bridge was instrumented by the same geophones as case 1 in three global directions to obtain the vibration measurements. The bridge was vibrated by dropping a 22.7 kg sandbag from a height of one meter at nine locations shown in Figure 3.10 on the bridge deck.

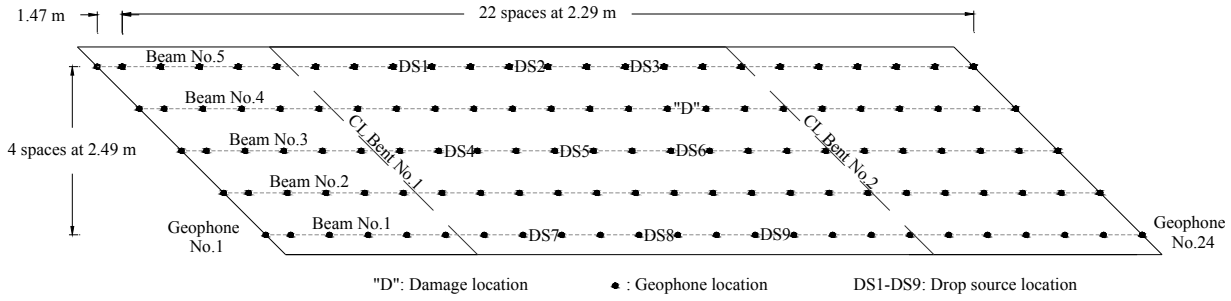

Figure 3.10. I-40 westbound bridge over 4th Avenue: geophone layout (modified from Ragland et al. 2011)

Data was recorded at a total of 120 geophone locations with a sampling rate of 1000 Hz for a total of 3 seconds using the 48-channel seismograph. The 120 measurement locations were

divided into five groups along the beam lines. For each group of sensors, the sandbag was dropped and the vertical and transverse vibration data were recorded; then, the horizontal sensors were rotated by 90° and the sandbag was dropped again to obtain the vertical and longitudinal vibration data. Once the data was recorded for all the three directions, the line of sensors were shifted to the next beam line and the tests were repeated until all the 120 measurement locations were covered. The same damage scenarios mentioned earlier for case 1 were implemented for this bridge as well and the vibration data corresponding to the bottom flange plus half of the web cut is used for the analysis. For this case, damage was located on an interior girder close to a support to further study the effectiveness of damage identification techniques for cases where damage is near a support as it is expected that vibration-based damage detection is less reliable at locating the damage occurring near a support (Zhou et al. 2007).

3.4.2.2. Data analysis and results

The same damage identification procedure mentioned earlier for case 1 is repeated here for the triaxial vibration data of I-40 westbound bridge over 4th Avenue obtained from nine drop source locations shown in Figure 3.10 and the analysis results are summarized in Table 3.3.

As shown in Table 3.3, the implemented damage identification technique has successfully detected the damage located on an interior girder near a support. It is seen that all the triaxial vibration data obtained from mainly vertical excitation source are able to detect the damage occurred on an interior girder near a support. However, none of them can locate the damage spatially or on the damaged beam. Compared with case 1 in which damage was located

at mid-span of an exterior girder, it is seen that when damage is located on an interior girder near a support, the chance of spatially locating the damage is considerably decreased.

Table 3.3. Damage identification results summary for the I-40 westbound bridge over 4th Avenue

Drop Source Location	Data Set No.	Vibration Component		
		Longitudinal	Transverse	Vertical
DS1	1	N/A	□	□
	2	□	N/A	□
DS2	1	N/A	□	○
	2	□	N/A	□
DS3	1	N/A	□	□
	2	□	N/A	□
DS4	1	N/A	□	□
	2	□	N/A	□
DS5	1	N/A	□	□
	2	□	N/A	□
DS6	1	N/A	□	□
	2	□	N/A	○
DS7	1	N/A	□	□
	2	○	N/A	□
DS8	1	N/A	□	□
	2	□	N/A	□
DS9	1	N/A	□	□
	2	○	N/A	□

●Damage spatially located; ○ Damage located on the damaged beam;
□ Damage detected but not located; --- Damage not detected; N/A data is not available

3.5. Summary and conclusions

This study presents a new damage identification technique for bridge structures using a drop weight source, inexpensive geophones and time series analysis. The vibration data obtained from drop test and recorded by geophones are corrected with regard to the geophones properties and then convolved with random values to simulate the tests for random loading. Several sensor clusters are defined along the structure and ARX models are created for each cluster in healthy condition of the structure. These ARX models are used for the data obtained in damaged

condition of the structure and convolved with random values to calculate the prediction errors. A new damage-sensitive feature is defined as the ratio of the standard deviations of the prediction errors to identify the existence and location of the damage. An outlier analysis method is used to identify the existence of damage. The validity of the proposed technique is demonstrated by using the triaxial vibration data of two full-scale bridges subjected to a controlled damage scenario induced to the bridge girder. The damage identification technique is repeated for the three global directions to investigate the efficacy of each longitudinal, transverse, and vertical vibration on structural health monitoring of the bridges.

- The results of the analysis for the two test bridges indicate that the proposed damage identification technique can identify the existence of damage in real-life bridges, even when damage is located at an obscure position such as on an interior girder near a support. The triaxial analysis results show that all triaxial vibrations have the ability to identify the damage when the main excitation source on the bridge is vertical.

- The damage localization results on a three-girder bridge in which damage was induced at a simple position, at mid-span of an exterior girder, show that damage cannot be consistently located. No success is found in locating the damage using the horizontal vibrations when the excitation source is applied mainly vertically but it is seen that a few vertical data sets can spatially locate the damage. Therefore, it seems that when bridge is excited mainly vertically, vertical vibrations are better choices for lining up the unidirectional sensors.

- The damage localization results on a five-girder bridge damaged at an obscure position, on an interior girder near a support, and excited mainly vertically show that damage cannot be located regardless of the vibration orientation.

3.6. Acknowledgments

The authors would like to acknowledge Drs. William S. Ragland, Richard T. Williams, Vasileios Maroulas, Husheng Li, and Mongi A. Abidi and Ali Taalimi at the University of Tennessee, Knoxville for their technical support and guidance.

3.7. References

Cheung, A., Cabrera, C., Sarabandi, P., Nair, K.K., Kiremidjian, A. and Wenzel, H. (2008). "The application of statistical pattern recognition methods for damage detection to field data." *Smart Mater. Struct.*, 17 (6), 065023.

Farrar, C.R. and Worden, K. (2007). "An introduction to structural health monitoring." *Phil. Trans. R. Soc. A*, 365, 303-315.

Fasel, T.R., Gregg, S.W. , Johnson, T.J., Farrar, C.R. and Sohn, H. (2002). "Experimental modal analysis and damage detection in a simulated three story building." *Proc. 20th IMAC Conference on Structural Dynamics*, Los Angeles, CA.

Gul, M. and Catbas, F. N. (2011a). "Structural health monitoring and damage assessment using a novel time series analysis methodology with sensor clustering." *J. Sound Vib.*, 330(6), 1196-1210.

Gul, M. and Catbas, F.N., (2011b). "Damage assessment with ambient vibration data using a novel time series analysis methodology." *J. Struct. Eng.*, 137(12), 1518-1526.

Kramer, C., De Smet, C. A. M., and De Roeck, G. (1999). "Z24 bridge damage detection tests." *Proc. 17th Int. Modal Analysis Conf. (IMAC XXVII)*, Society for Experimental Mechanics (SEM), Bethel, CT, 1023–1029.

Ljung, L. (1999). *System identification: theory for the user*, second ed., Prentice-Hall, Upper Saddle River, NJ.

Lu, Y., and Gao, F. (2005). "A novel time-domain auto-regressive model for structural damage diagnosis." *J. Sound Vib.*, 283(3–5), 1031–1049.

MATLAB version 7.12 [Computer software]. (2011). The MathWorks Inc., Natick, MA.

Nair, K. K., Kiremidjian, A. S., and Kincho, H. L. (2006). "Time series-based damage detection and localization algorithm with application to the ASCE benchmark structure." *J. Sound Vib.*, 291 (1–2), 349–368.

Omenzetter, P., and Brownjohn, J. M. (2006). "Application of time series analysis for bridge monitoring." *Smart Mater. Struct.*, 15(1), 129–138.

Ragland, W. S. (2009). "Structural health monitoring and damage evaluation of full-scale bridges using triaxial geophones: controlled in-situ experiments and finite element modeling." Ph.D. Dissertation, Dept. of Civil and Environmental Engineering, University of Tennessee, Knoxville, TN.

Ragland, W. S., Penumadu, D. and Williams, R. T. (2010). "Using geophones for nondestructive evaluation of full-scale bridges." *Transp. Res. Rec.*, Transportation Research Board, No. 2201, 45–52.

Ragland, W. S., Penumadu, D. and Williams, R. T. (2011). "Finite element modeling of a full-scale five-girder bridge for structural health monitoring." *Struct. Health Monit.*, 10(5), 449-465.

Sohn, H. and Farrar, C.R. (2001). "Damage diagnosis using time series analysis of vibration signals." *Smart Mater. Struct.*, 10(3), 446- 451.

Worden, K., Manson, G., and Fieller, N. J. (2000). "Damage detection using outlier analysis." *J. Sound Vib.*, 229 (3), 647-667.

Zhou, Z, Wegner, L. D. and Sparling, B.F. (2007). "Vibration-based detection of small-scale damage on a bridge deck." *J. Struct. Eng.*, 133(9), 1257–1267.

Chapter 4. Dynamic Analysis and Damage Identification of a Full-Scale Bridge Excited by a Drop Weight

Reza Vasheghani-Farahani and Dayakar Penumadu

My primary contributions to this chapter included: (1) gathering and reviewing literature, (2) developing and calibrating finite element model of the bridge for modal analysis and then explicit dynamic analysis (3) writing and developing MATLAB codes for implementing time-series based damage identification technique, (4) adapting an outlier analysis method to detect the damage, and (5) most of the writing.

4.1. Abstract

Recently tested a full-scale five-girder damaged bridge excited by a drop weight indicated that dynamic properties of the bridge did not significantly change after inducing the damage on an interior girder near a support while vibration-based damage identification techniques are typically based on the premise that dynamic characteristics of a structure change after the occurrence of a damage. This study presents finite element (F.E.) analysis of the bridge to verify the effect of damage to the bridge girder on the dynamic properties of the bridge and also to investigate the effects of damage location and extent, efficacy of each triaxial vibration, and additive noise to the vibration data on the vibration-based damage identification technique. Autoregressive with exogenous input (ARX) models and sensor clustering damage identification technique is used to identify the induced damage from vibration data obtained from F.E. models. The analysis results indicate that dynamic properties of the bridge do not significantly change after inducing the damage occurred near a support but the implemented damage identification technique can still detect the damage. Damage identification results show that for the bridge vibrated vertically: (1) the implemented technique can detect and locate the damage occurred at mid-span of an exterior girder for various damage levels (2) when damage is located near a support on an interior girder, damage is detected but not located (3) all the triaxial vibration data can be used to detect the damage but vertical vibration data is the best option to locate the damage (4) Additive noise to the vibration data reduces the damage localization resolution (5) the implemented damage identification technique can be still used to identify multi-damage scenarios if damage level is large.

4.2. Introduction

One of the main objectives of Structural Health Monitoring of bridges is damage identification and integrity assessment (Zhang 2007). A variety of damage identification techniques have been proposed based on the premise that changes in the dynamic characteristics of a structure can be used as an indicator of damage or deterioration (Doebling et al. 1998). One of the common damage identification techniques is time series-based damage identification technique which relies on the fact that when a time series model approximates the vibration response of a structure and model coefficients or residual error are obtained, any deviations in these coefficients or residual error can be inferred as an indication of a change or damage in the structure. Several time series-based damage identification algorithms have been proposed and developed by different researchers to extract damage-sensitive features which can identify the damage (Gul and Catbas 2011a,b, Lu and Gao 2005, Nair et al. 2006, Omenzetter and Brownjohn 2006, Sohn and Farrar 2001). For example, Lu and Gao (2005) presented a new method for damage diagnostic based on linear dynamic equations and formulated in the form of autoregressive with exogenous input (ARX) model. They used the standard deviation of the residual error which was the difference between the measured signals from any state of the system and the predicted signals from the ARX model created from a reference state, as damage-sensitive feature. They used two numerical mass-spring systems and indicated that their approach was successful to detect and locate the damage. Recently, ARX models and sensor clustering technique has been used for damage identification (Gul and Catbas 2011a,b). In this technique, ARX models are created for sensor clusters in healthy condition of the structure; then, these models are used for the data obtained in damaged condition of the structure to estimate the

damage-sensitive features. Gul and Catbas (2011a) used the ARX models and sensor clustering damage identification method for ambient vibration data to detect and locate the damage. They defined a fit ratio based on the norms of measured output minus predicted output and measured output minus mean of measured output and used the difference between the fit ratios of the models in healthy and damaged conditions of the structure as a damage-sensitive feature. They applied this technique to a laboratory steel grid structure subjected to different damage scenarios and indicated that damage was detected and located for most of the cases. They also used the data from Z24 bridge (Kramer et al. 1999) where different levels of pier settlement were applied as damage and showed that damage was detected and located with a minimum number of false alarms.

In real-life bridge monitoring, environmental and operational effects; such as changes in temperature (Peeters and Roeck 2001) and noise (Zhang 2007), can make the use of vibration based-damage identification techniques difficult since they can affect the dynamic characteristics of a bridge similar to the damage. Moreover, it has been shown that fundamental frequencies and mode shapes of real-life bridges may not significantly influenced by local damage (Ragland 2009, Ragland et al. 2011). All of these facts invoke the need for some simplified studies of full-scale bridges to better understand the factors that can affect dynamic characteristics of the bridge and subsequently the ability of vibration-based damage identification techniques to identify the damage.

This study presents F.E. analysis of a full-scale five-girder bridge excited by a drop weight on the bridge deck to obtain simulated vibration data for varying single-damage and multi-damage scenarios including those not imposed during the field tests to see if the induced

damage can be identified by vibration-based damage identification techniques for different levels of noise in the vibration data. It also investigates the efficacy of each triaxial vibration component in identifying the induced damage. The bridge considered in this study is a common bridge type in the U.S.; therefore, the obtained results can be applicable to a large number of bridges.

4.3. Description of the bridge

The I-40 westbound bridge over 4th Avenue was constructed in 1967 in Knoxville, TN. It was a 45° skewed bridge consisting of three spans supported by five steel girders as shown in Figures 4.1 and 4.2. This bridge was used for evaluating the feasibility of vibration-based damage identification techniques when damage was located near a support for a highly structurally redundant bridge with very high chance of re-distribution of external loads.

Figure 4.1. Photo of the I-40 westbound bridge over 4th Avenue

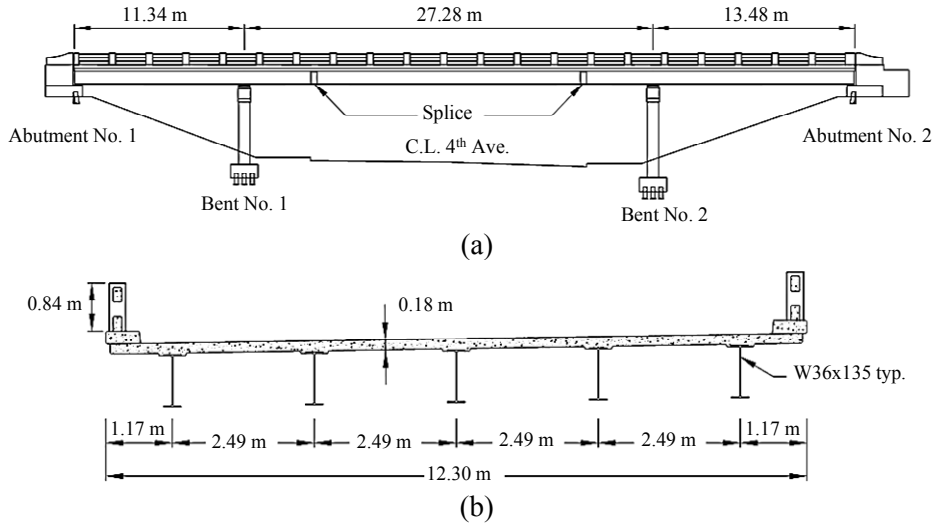

Figure 4.2. I-40 westbound bridge over 4th Avenue: (a) Longitudinal profile (b) Cross-section (modified from Ragland 2011)

The bridge was excited by dropping a 22.7 kg sandbag from a height of one meter at nine locations shown in Figure 4.3. Data was recorded at a total of 120 sensor locations shown in Figure 4.3 with a sampling rate of 1000 Hz for a total of 3 seconds.

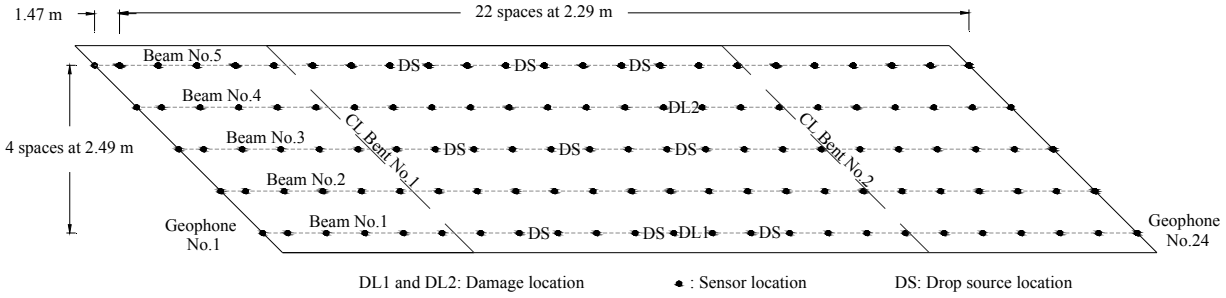

Figure 4.3. I-40 westbound bridge over 4th Avenue: sensor layout (modified from Ragland et al. 2011)

During the field tests, three damage scenarios shown in Figure 4.4 were applied to an interior girder close to a support, DL2 location shown in Figure 4.3, to study the feasibility of vibration-

based damage identification techniques for cases where damage is near a support as it is expected that vibration-based damage detection is less reliable at locating the damage occurring near a support (Zhou et al. 2007).

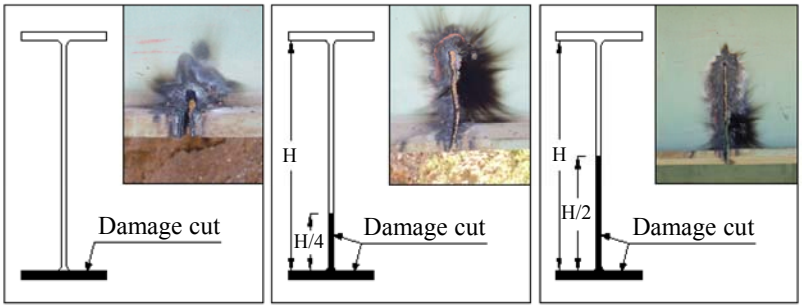

Figure 4.4. Induced damage scenarios: (a) Bottom flange cut (D1) (b) Bottom flange plus ¼ of the web cut (D2) (c) Bottom flange plus ½ the web cut (D3)

4.4. Finite element modeling of the test bridge

4.4.1. Description of the finite element model

In this study, linear elastic finite element (F.E.) model of the I-40 westbound bridge over 4th Avenue is generated using the commercial package ABAQUS version 6.9 (2009) as shown in Figure 4.5. In this model, all the elements are selected as shell elements except the bent columns and bracings which are beam elements and the sandbag which is solid element. Handrails are not modeled and an equivalent mass is added to the model instead. The model simulates composite action between the girders and the concrete slab by tying the top flange of each girder to the concrete slab directly above the girder. The bent columns are modeled as fixed at the ground surface and steel girders are modeled as simply supported at the ends. The bottom flanges of girders are so tied to the bents at the bent-girder connections that identical X, Y and Z

translations are obtained. To match the experimental data, the horizontal (X and Z) translations of the slab at the abutment locations are restrained.

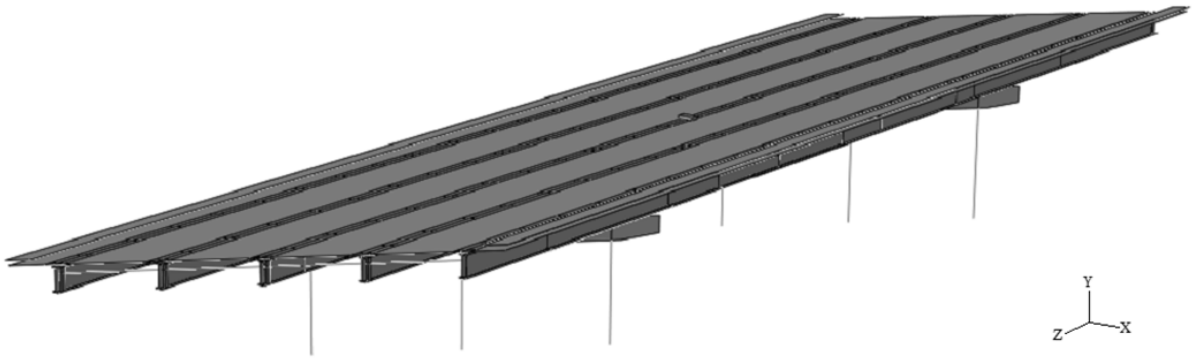

Figure 4.5. F.E. model of the I-40 westbound bridge over 4th Avenue subjected to a drop weight

The concrete and steel material properties used for the bridge elements are shown in Table 4.1. The concrete properties are defined based on the properties of the cores taken from the bridge deck.

Table 4.1. Concrete and Steel Material Properties for FEMs

Material	E(GPa)	Poisson's ratio	Density (kg/m3)
Concrete	22.3	0.2	2400
Steel	200	0.3	7850

4.4.2. Simulated damage scenarios

To simulate the damage scenarios induced during the field tests, the bridge girders are modeled as tied surfaces. These surfaces represent top flanges, webs and bottom flanges. Each of these surfaces is models as two independent parts at the damage location. For undamaged condition,

the two parts are tied together to have identical translational and rotational degrees of freedom at the damage location. The webs are so constructed at the damage location that nodes occur at the quarter and half points of the web so that damage scenarios D2 and D3 can be applied. To simulate damage scenario D1, the ties between bottom flanges at the damage location is untied which allow for independent translation and rotation of each part. Damage scenario D2 is simulated by untying the bottom flanges and the bottom quarter of the web parts at the damage location. Finally, damage scenario D3 is simulated by untying the bottom flanges and bottom half web parts at the damage location.

4.4.3. Finite element model verification

To verify the F.E. model of the bridge with the real bridge, modal analysis is carried out. The shell elements are selected as standard four-noded doubly curved shell with reduced integration, S4R, and beam elements are selected as standard three-noded quadratic beam in space, B32. The sandbag is removed from the F.E. model to do the modal analysis. The F.E. model is then verified by comparing its first three natural frequencies and mode shapes with those obtained from the field data. Table 4.2 presents natural frequencies obtained from the F.E. model and those measured from the test bridge for each damage scenario. As shown, a good agreement exists between the F.E. and measured frequencies.

Table 4.2. Fundamental natural frequencies identified from the field test and F.E. model

Damage Scenario		Mode 1	Mode 2	Mode 3
Undamaged	Field test	4.34	4.41	6.39
	F.E. model	4.27	4.40	6.48
	% Diff.	-1.61	-0.23	1.41
D1, Flange cut	Field test	4.35	4.44	6.35
	F.E. model	4.27	4.40	6.48
	% Diff.	-1.84	-0.90	2.05
D2, Flange + 1/4 web cut	Field test	4.29	4.43	6.38
	F.E. model	4.27	4.40	6.48
	% Diff.	-0.47	-0.68	1.57
D3, Flange + 1/2 web cut	Field test	4.26	4.40	6.40
	F.E. model	4.27	4.40	6.48
	% Diff.	0.23	0.00	1.25

To further verify the F.E. model of the bridge, Modal Assurance Criterion (MAC), shown in Eq. (4.1) for corresponding modes, is used to compare the first three mode shapes obtained from the F.E. model with those measured from the experimental tests.

$$\mathrm{MAC} = \frac{\left|\{\varphi_F\}^T \{\varphi_E\}\right|^2}{\left(\{\varphi_F\}^T \{\varphi_F\}\right)\left(\{\varphi_E\}\right)^T \{\varphi_E\}\right)} \tag{4.1}$$

where $\{\varphi_F\}$ is the F.E. modal vector and $\{\varphi_E\}$ is the experimental modal vector. The MAC value indicates the degree of correlation between the F.E. mode shape and the experimental mode shape and varies from 0 to 1. If the modes are identical, a value of one will be obtained while for two different modes, a value of zero will be attained. In general, a MAC value greater than 0.9 indicates well-correlated modes while a value less than 0.1 indicates uncorrelated modes (Ewins 2000).

To form the F.E. modal vectors and calculate the MAC, translational components in the X, Y, and Z directions are extracted from the F.E. model mode shapes at sensor locations for the first three modes and MAC values are calculated. Table 4.3 presents the MAC values comparing

the identified three first mode shapes from the F.E. models and the field tests for different damage scenarios.

Table 4.3. MAC results: Field tests vs. F.E. models

Damage scenario	Mode		
	1	2	3
Undamaged	0.96	0.92	0.96
D1	0.96	0.92	0.96
D2	0.96	0.92	0.96
D3	0.96	0.92	0.97

As shown in Table 4.3, good agreements exist between the F.E. modes and measured modes for all the damage scenarios indicating that the F.E. models accurately represent the three dimensional dynamic response of the bridge for healthy and damaged conditions.

4.4.4. Dynamic analysis

Vibration-based damage identification techniques are based on the dynamic response of structures measured before and after the damage occurs. To obtain dynamic response of the structure under the drop weight, dynamic explicit approach in ABAQUS is used. The shell elements are selected as explicit four-noded doubly curved shell with reduced integration, small membrane strains, and warping in small-strain formulation, S4RSW, and the beam elements are selected as explicit three-noded quadratic beam in space, B32, and solid element is selected as explicit 8-node linear brick with reduced integration, C3D8R. The sandbag is modeled just above the impact surface and an initial velocity reflecting the drop height of 1 meter is applied to the sandbag. The gravitational acceleration is applied to the sandbag.

4.5. Damage identification procedure

In this study, ARX models and sensor clustering damage identification technique (Gul and Catbas 2011a,b) is used mainly because of its simplicity and promising results on the Z24 bridge data (Gul and Catbas 2011a). Similar results are obtained when the developed ARX models and sensor clustering approach, explained in Chapter 2, is used. The vibration data are normalized according to Eq. (4.2) to be comparable at a sensor location:

$$v_i(t) = \frac{\hat{v}_i(t) - \mu_i}{\sigma_i} \tag{4.2}$$

where $\hat{v}_i$ is the velocity of geophone i and v_i is the normalized velocity of geophone i. μ_i and σ_i are mean and standard deviation of the velocity of geophone i, respectively. When data are normalized, several sensor clusters are created along each bridge beam line and ARX models shown in Eq. (4.3), are created for each cluster in healthy condition of the bridge.

$$A(q)v_r(t) = B(q)v(t) + e(t) \tag{4.3}$$

where $v_r(t)$ is the velocity response at the reference sensor of a cluster, and $v(t)$ is the matrix of velocity responses of the sensors inside the cluster. This methodology is illustrated in Figure 4.6 for a bridge girder with 24 sensors.

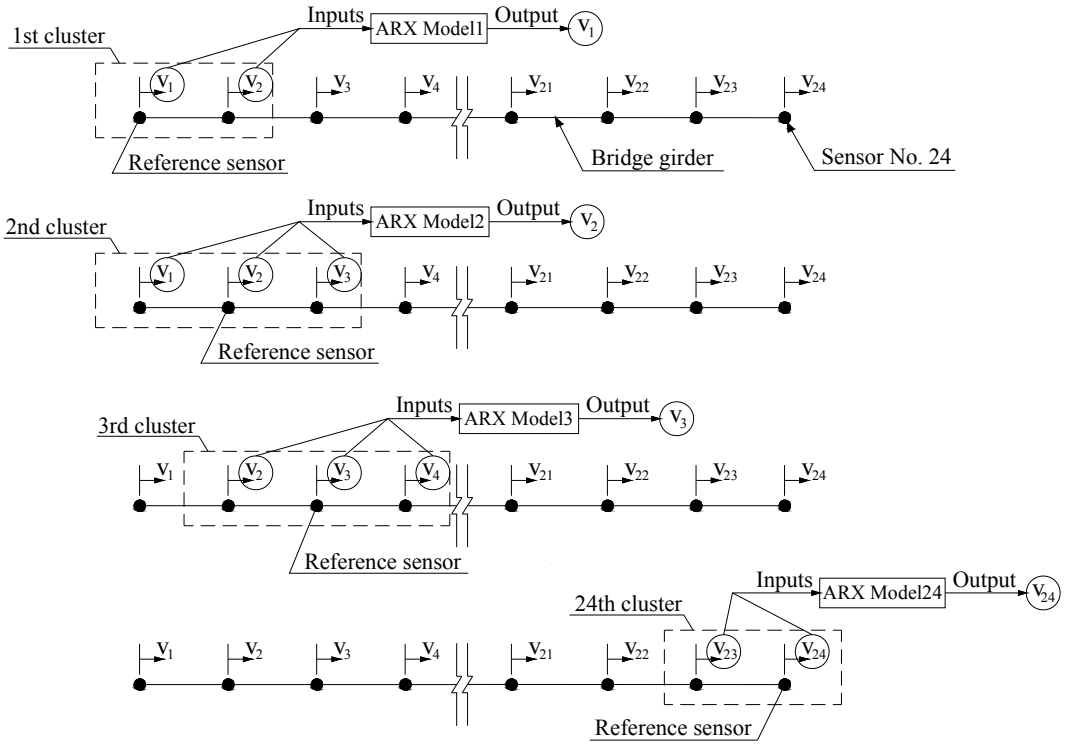

Figure 4.6. Creating ARX models for different sensor clusters along a beam with 24 sensors

As shown, for a girder with 24 sensors, 24 clusters are defined having one reference sensor each. The first cluster includes two sensors, the reference sensor and the sensor next to it. For the second cluster, there are three sensors in which the middle one is considered as the reference sensor. Clusters 3-23 are defined similarly to the second cluster. The last cluster is defined similarly to the first cluster where the reference sensor is the last sensor. For each of these clusters, the inputs to the ARX model are the outputs of the sensors in the cluster, while the ARX model output is the output of the reference sensor.

After creating the ARX models in healthy condition of the bridge, these models are used for the data obtained in damaged conditions to estimate the prediction errors, e_p. Damage-sensitive features (DSFs) are defined as the ratio of the standard deviation of the prediction error

in damaged condition to the standard deviation of the prediction error in healthy condition of the bridge. To identify the damage, an outlier analysis method is used. A threshold is defined by using damage-sensitive features obtained in healthy condition of the structure above which the structure is considered as damaged.

4.6. Sensitivity analysis for damage identification

This study investigates the effects of damage location and extent, efficacy of each triaxial vibration, and additive noise to the vibration data on the vibration-based damage identification technique. It also studies multi-damage scenarios to see if the implemented damage identification technique can identify the damage.

4.6.1. Effects of damage location and extent

To investigate the effects of damage location and extent on the vibration-based damage identification, two cases are studied: (1) damage is located at mid-span of an exterior girder and (2) damage is located on an interior girder near a support.

4.6.1.1. Damage located at mid-span of an exterior girder

The vertical vibration data obtained from F.E. models is first normalized according to Eq. (4.2). 24 sensor clusters are defined along each girder line and ARX models are created for each cluster in healthy condition of the bridge. In order to determine the suitable ARX model orders, first maximum model orders are set to 3 to prevent any overfeeding. Then the vibration data obtained from the healthy condition of the structure is split to two parts, where the first part is used for the

estimation and the second part is used for the validation. The best model is then selected by comparing the output of the models with orders ranging between 1 and 3 with the validating data (MATLAB 2011). The ARX models determined in healthy condition of the bridge are used for the data obtained in damaged condition to find the prediction errors and to calculate the damage-sensitive features. Figure 4.7 shows the results of the damage identification for noise free vertical vibration data obtained under different damage levels.

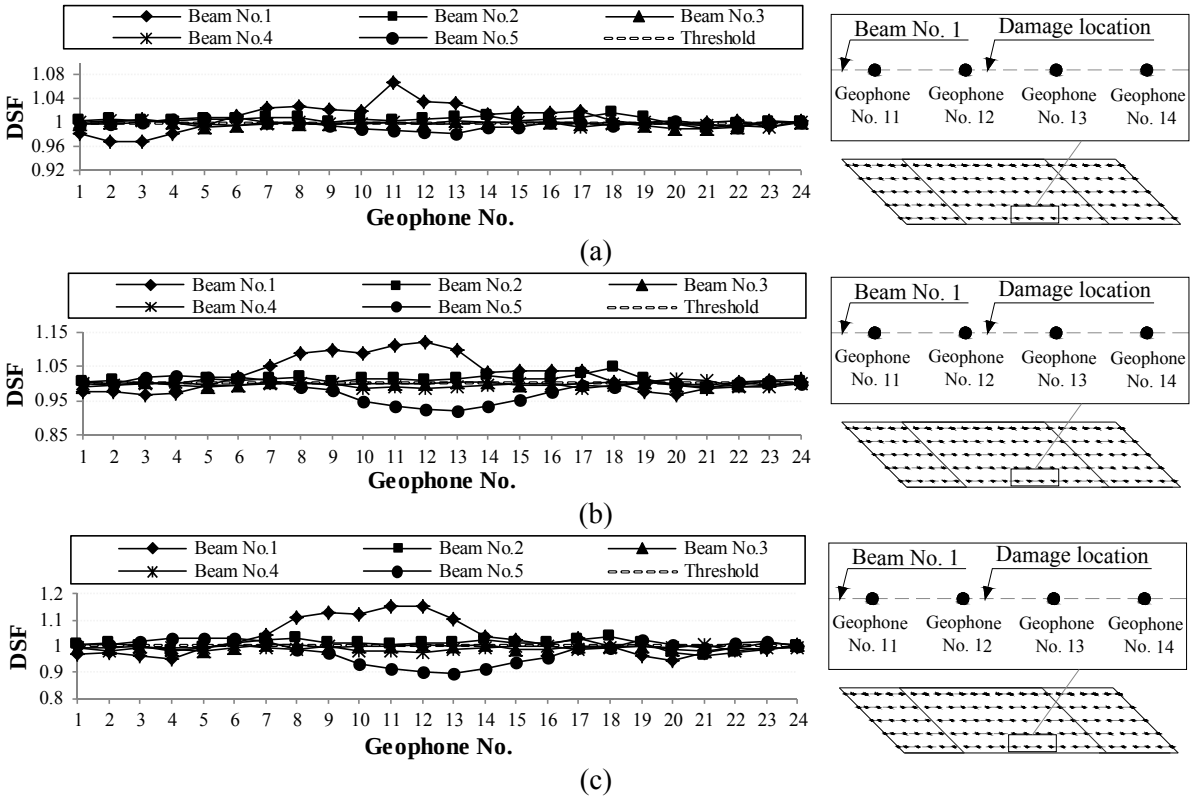

Figure 4.7. Damage identification results for noise free vertical vibration data when damage is located at DL1 (a) Damage scenario D1 (b) Damage scenario D2 (c) Damage scenario D3

As can be seen, the implemented damage identification technique can detect the induced damage even for small level of damage when damage is located at mid-span of an exterior

girder. It is also seen that the implemented technique is able to locate the damage for noise free data when damage is located at mid-span of an exterior girder.

4.6.1.2. Damage induced on an interior girder near a support

The procedure mentioned above is repeated for the case that damage is located on an interior girder near a support (DL2 location shown in Figure 4.3) to see if the implemented technique can still detect and locate the damage. Figure 4.8 presents the results of the analysis using the vertical noise free vibration data for different damage levels.

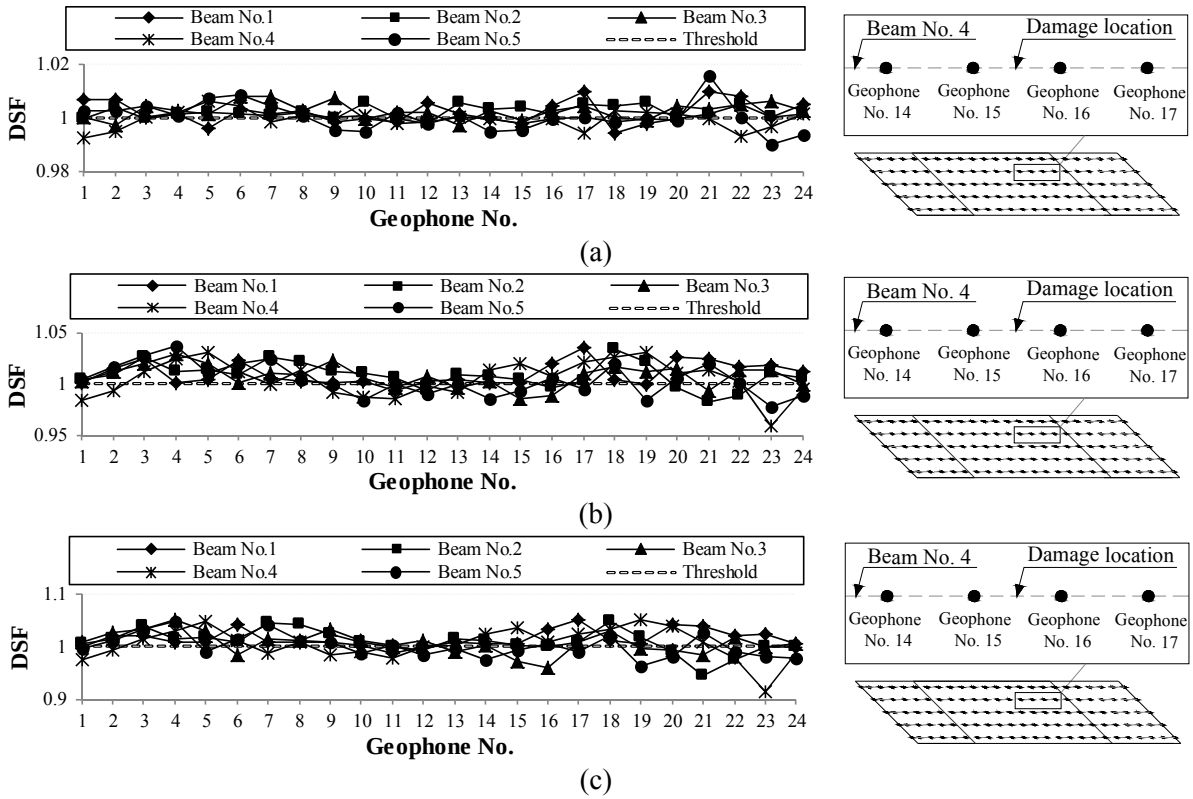

Figure 4.8. Damage identification results for noise free data vertical vibration when damage is located at DL2 (a) Damage scenario D1 (b) Damage scenario D2 (c) Damage scenario D3

As shown, the implemented damage identification technique can successfully detect the damage occurred on an interior girder near a support even when damage level is small; however, it cannot locate the damage.

4.6.2. Efficacy of each triaxial vibration on damage identification

To investigate the effect of each triaxial vibration data on damage identification of bridges, the aforementioned technique is implemented independently in three global directions. Table 4.4 presents the results of the analysis for longitudinal, transverse and vertical vibration data. Here, longitudinal refers to the bridge length direction whereas transverse refers to the direction perpendicular to the bridge length.

Table 4.4. Damage identification results for the I-40 westbound bridge over 4th Avenue

Damage location	Damage scenario	Vibration Component		
		Longitudinal	Transverse	Vertical
DL1	D1	○	○	●
	D2	□	□	●
	D3	□	○	●
DL2	D1	□	□	□
	D2	□	□	□
	D3	□	□	□

●Damage spatially located; ○ Damage located on the damaged beam;
□ Damage detected but not located; --- Damage not detected

As shown in Table 4.4, when the excitation source is vertical, all the vibration data are able to identify the existence of damage even when damage is small and located on an interior girder near a support. It is seen that when damage is located at mid-span of an exterior girder, the vertical vibration data are able to identify the spatial location of the damage even when damage

is small. As shown, no success is found in locating the damage occurred on an interior girder near a support.

4.6.3. Effect of additive noise to the vibration data

To further investigate the implemented damage identification technique for noisy data, 10% white Gaussian noise is added to the vertical vibration data obtained from the F.E. models and damage identification technique is performed. To define the threshold level, an outlier analysis method is adapted similar to Worden et al. (2000) and Gul and Catbas (2011b) where a Monte Carlo method was used. First, 10% white Gaussian noise is added to the vertical vibration data obtained in healthy condition of the structure at various sensor locations and damage-sensitive features (DSFs) are calculated. The process is repeated many times and DSFs are saved (in this study, the process is so repeated that 1000 DSFs are saved). The DSFs are sorted and the value above which only 5% of the simulations occur is selected as the threshold value, over which the bridge structure can be considered as damaged.

4.6.3.1. Damage located at mid-span of an exterior girder

In this case, 10% white Gussian noise is added to the vertical vibration data obtained from the F.E. models for various damage levels and damage identification technique is performed. Figure 4.9 shows the results of the damage identification for different damage levels occurred at mid-span of an exterior girder (DL1 location shown in Figure 4.3) for noisy data.

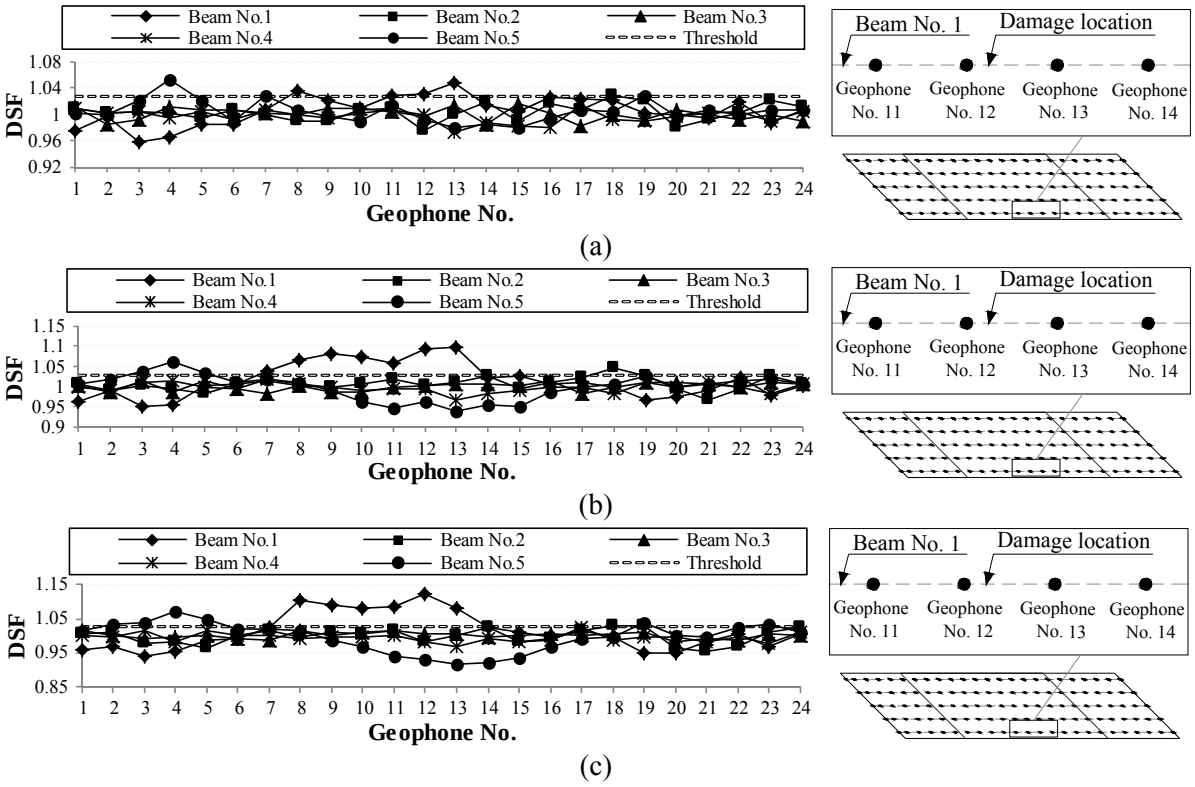

Figure 4.9. Damage identification results for noisy vertical vibration data when damage is located at DL1 (a) Damage scenario D1 (b) Damage scenario D2 (c) Damage scenario D3

As can be seen, for vibration data with 10% additive white Guassian noise, the implemented technique can still identify the existence and spatial location of the damage occurred at mid-span of an exterior girder when damage extent is large. In Figure 4.9(a) in which damage extent is small, it is seen that the location of the induced damage is not correctly identified due to the added noise to the vibration data.

4.6.3.2. Damage located on an interior girder near a support

Similar analysis is repeated for the case that damage is located on an interior girder near a support, DL2 location shown in Figure 4.3, and the results are presented in Figure 4.10 for different damage extents.

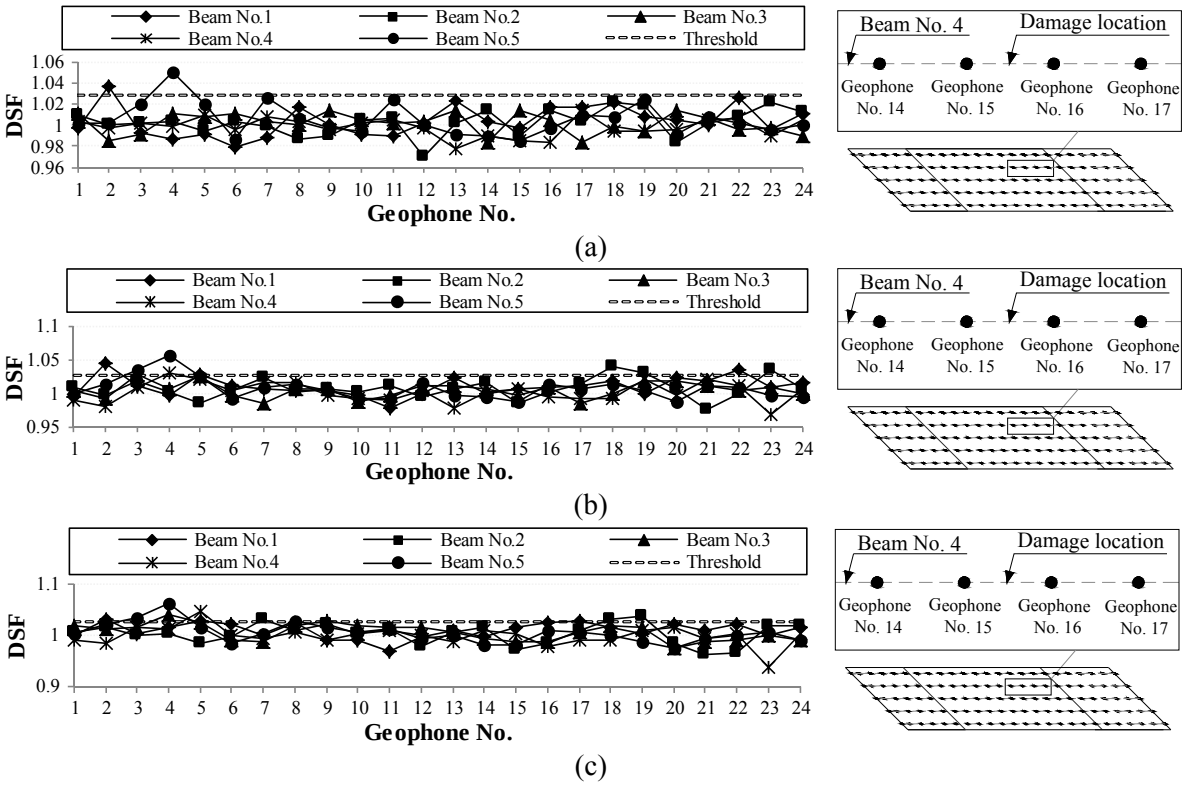

Figure 4.10. Damage identification results for noisy vertical vibration data when damage is located at DL2 (a) Damage scenario D1 (b) Damage scenario D2 (c) Damage scenario D3

As can be seen, for vibration data with 10% additive white Guassian noise, the implemented damage identification technique can still identify the existence of damage occurred on an interior girder near a support even for small damage levels; however, no success is found in locating the damage.

4.6.4. Multi-damage scenarios

To investigate the feasibility of the implemented damage identification technique for the cases that damage exists in more than one location, in this section both damage locations studied before, DL1 and DL2 shown in Figure 4.3, are considered simultaneously for the three damage scenarios mentioned earlier. The ARX models and sensor clustering damage identification technique is repeated for noise free and noisy vertical vibration data in which 10% white Gaussian noise is added to the data and the results are presented in Figures 4.11 and 4.12, respectively.

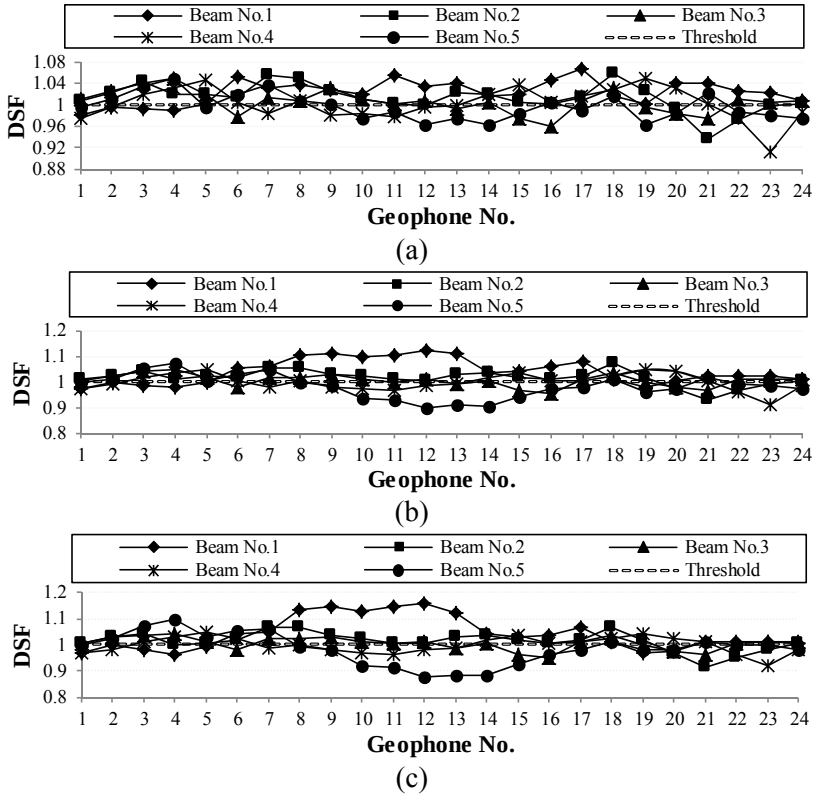

Figure 4.11. Damage identification results for noise free vertical vibration data when damage is occurred simultaneously at DL1 and DL2 (a) Damage scenario D1 (b) Damage scenario D2 (c) Damage scenario D3

From Figure 4.11, it is seen that the implemented damage identification technique can still be used to detect and locate the multi-damage scenarios if the damage level is large. However, the damage occurred near a support on an interior girder cannot be still located. From Figure 4.11(a), it is clear that when damage level is small, the implemented damage identification technique can detect the damage but it cannot identify the spatial location of the damage.

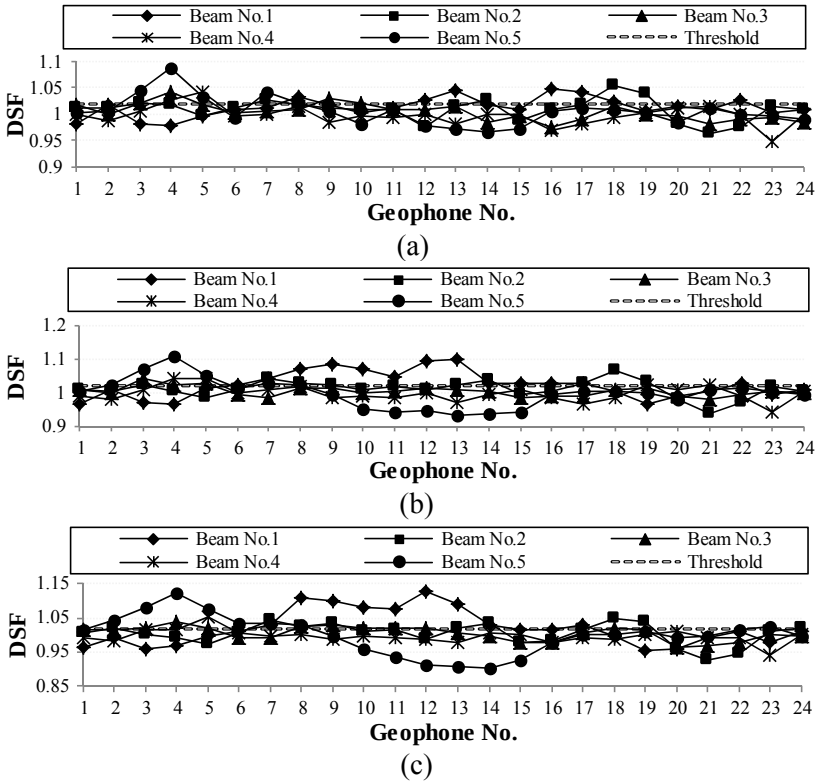

Figure 4.12. Damage identification results for noisy vertical vibration data when damage is occurred simultaneously at DL1 and DL2 (a) Damage scenario D1 (b) Damage scenario D2 (c) Damage scenario D3

From Figure 4.12, it is seen that when data are noisy, the implemented damage identification technique can still detect and locate the damage if damage level is large. When

damage level is small, the implemented technique can detect the damage but it cannot locate the damage correctly. As shown, by increasing the extent of induced damage, the resolution of damage localization is improved.

4.7. Summary and Conclusion

This study presents finite element analysis of a full-scale five-girder bridge subjected to controlled levels of known damage on the bridge girders and excited by a drop weight on the bridge deck. The F.E. model of the bridge is calibrated using dynamic response of the bridge already obtained using an array of dense sensors. Modal analysis is performed on the F.E. model to obtain natural frequencies and mode shapes to compare with those obtained from the field data. After calibrating the F.E. model of the bridge, dynamic explicit analysis is performed to simulate the experimental tests and to obtain vibration signals. Several damage scenarios are considered for finite element analysis including those not imposed during the field tests. Autoregressive with exogenous input (ARX) models and sensor clustering damage identification technique is used to obtain prediction errors in healthy and damaged conditions of the bridge. A new damage-sensitive feature is defined as the ratio of the standard deviation of the prediction error in damaged condition to the standard deviation of the prediction error in healthy condition of the bridge to identify the existence and location of damage. The analysis results indicate that dynamic properties of the bridge do not significantly change after inducing the damage occurred on an interior girder near a support but the implemented damage identification technique can still detect the damage even when damage level is small. It is seen that the implemented technique can detect and spatially locate the damage even for small damage level when it is occurred at

mid-span of an exterior girder. It is also seen that additive noise to the vibration data, reduces the resolution of damage localization. For small damage levels, adding 10% white Gaussian noise to the vibration data causes the location of damage not to be correctly identified while for larger damage levels, the implemented technique can still locate the damage. It is also shown that for the bridge vibrated vertically, all the triaxial vibration data can be used to detect the damage; however, just vertical vibration data can locate the damage occurred at mid-span of an exterior girder. It is seen that for damage located on an interior girder near a support, none of the triaxial vibration data can locate the damage. The multi-damage analysis results indicate that the implemented damage identification technique can be still used to detect and locate the damage if damage level is large. However, it cannot locate the damage occurred near a support on an interior girder.

4.8. Acknowledgments

The authors are grateful for accessing to Dr. William S. Ragland's finite element model files for verifying and developing the finite element models used in this study. The authors would also like to acknowledge Dr. Wenchao Song and Dr. James A. Mason for their technical support and guidance.

4.9. References

ABAQUS version 6.9 [Computer software]. (2009). Dassault Systèmes Simulia Corp., Providence, RI.

Doebling, S.W., Farrar, C.R., and Prime, M.B. (1998). "A summary review of vibration-based damage identification methods." *Shock Vib. Dig.*, 30(2), 91–105.

Ewins, D. J. (2000). "Model validation: correlation for updating." *Sadhana*, 25(3), 221–234.

Gul, M. and Catbas, F.N., (2011a). "Damage assessment with ambient vibration data using a novel time series analysis methodology." *J. Struct. Eng.*, 137(12), 1518-1526.

Gul, M. and Catbas, F. N. (2011b). "Structural health monitoring and damage assessment using a novel time series analysis methodology with sensor clustering." *J. Sound Vib.*, 330(6), 1196-1210.

Kramer, C., De Smet, C. A. M., and De Roeck, G. (1999). "Z24 bridge damage detection tests." *Proc., 17th Int. Modal Analysis Conf. (IMAC XXVII)*, Society for Experimental Mechanics (SEM), Bethel, CT, 1023–1029.

Lu, Y., and Gao, F. (2005). "A novel time-domain auto-regressive model for structural damage diagnosis." *J. Sound Vib.*, 283(3–5), 1031–1049.

MATLAB version 7.12 [Computer software]. (2011). The MathWorks Inc., Natick, MA.

Nair, K. K., Kiremidjian, A. S., and Kincho, H. L. (2006). "Time series-based damage detection and localization algorithm with application to the ASCE benchmark structure." *J. Sound Vib.*, 291 (1–2), 349–368.

Omenzetter, P., and Brownjohn, J. M. (2006). "Application of time series analysis for bridge monitoring." *Smart Mater. Struct.*, 15(1), 129–138.

Peeters, B. and Roeck, GD. (2001). "One-year monitoring of the Z24-Bridge: environmental effects versus damage events." *Earthquake Eng Struct Dyn,* 30(2), 149–71.

Ragland, W. S. (2009). "Structural health monitoring and damage evaluation of full-scale bridges using triaxial geophones: controlled in-situ experiments and finite element modeling." Ph.D. Dissertation, Dept. of Civil and Environmental Engineering, University of Tennessee, Knoxville, TN.

Ragland, W. S., Penumadu, D. and Williams, R. T. (2011). "Finite element modeling of a full-scale five-girder bridge for structural health monitoring." *Struct. Health Monit.*, 10(5), 449-465.

Sohn, H. and Farrar, C.R. (2001). "Damage diagnosis using time series analysis of vibration signals." *Smart Mater. Struct.*, 10(3), 446- 451.

Worden, K., Manson, G., and Fieller, N. J. (2000). "Damage detection using outlier analysis." *J. Sound Vib.*, 229 (3), 647-667.

Zhang, Q.W. (2007). "Statistical damage identification for bridges using ambient vibration data." Comput. Struct., 85(7-8), 476-485.

Zhou, Z, Wegner, L. D. and Sparling, B.F. (2007). "Vibration-based detection of small-scale damage on a bridge deck." *J. Struct. Eng.*, 133(9), 1257–1267.

Chapter 5: Conclusions and suggestions for future works

5.1. Conclusions

This study presents innovative techniques for damage identification of bridge structures using a controlled drop weight source, an inexpensive array of geophones, and a time series analysis. The most significant observations made from this study from analysis of vibration data obtained from real-life bridges and also from finite element simulations of a real-life bridge are as follows:

- The implemented time series-based damage identification techniques, AR-ARX and ARX models and sensor clustering, are able to identify the existence of damage in real-life bridges, even when the damage level is small and damage is located at an obscure position such as near a support on an interior girder.

- The implemented time series-based damage identification techniques cannot consistently locate the damage in real-life bridges. It is seen that when damage is located on an interior girder near a support, the chance of locating the damage is considerably reduced.

- The analysis results using triaxial vibration data obtained from real-life bridges under vertical excitation source indicate that all the triaxial vibration data are able to detect the damage.

- No success is found in locating the damage using the horizontal vibration data when the excitation source is applied mainly vertically, but it is seen that a few vertical data sets can spatially locate the damage. Therefore, it seems that when a bridge is excited mainly vertically, vertical vibration data is a better choice for lining up the unidirectional sensors.

- The damage localization results on a five-girder bridge damaged at an obscure position, on an interior girder near a support, and excited mainly vertically show that damage cannot be located regardless of the vibration data used.

- The finite element (F.E.) analysis results indicate that dynamic properties of the bridge do not significantly change after inducing the damage occurred on an interior girder near a support, but the ARX models and sensor clustering damage identification technique can still detect the damage even when damage level is small.

- The damage identification results, based on the vertical vibration data obtained from the F.E. models, indicate that damage which occurred at mid-span of an exterior girder could be detected and located.

- The damage identification results, based on the vibration data obtained from the F.E. models, indicate that additive noise to the vibration data reduces the resolution of damage localization. It is seen that, for small damage levels, adding 10% white Gaussian noise to the vibration data causes the location of damage not to be correctly identified, while for large damage levels, the implemented technique can still locate the damage.

- The damage identification results using the triaxial vibration data obtained from the F.E. models indicate that for the bridge vibrated vertically, all the triaxial vibration data can be used to detect the damage; however, vertical vibration data can alone locate the damage which occurred at mid-span of an exterior girder.

- The damage identification results, based on the vibration data obtained from the F.E. models, indicate that for damage located on an interior girder near a support, none of the triaxial vibration data can locate the damage.

- The multi-damage analysis results using the vibration data obtained from F.E. models indicate that ARX models and sensor clustering damage identification technique can be used to detect and locate the damage if damage level is large. However, it cannot locate the damage occurred near a support on an interior girder. It is seen that for small damage levels, the implemented damage identification technique can detect the damage but it cannot locate the damage.

5.2. Suggestions for future works

Based on the analysis presented in this dissertation, some areas of possible future work are:

- The damage identification results from the signals obtained from the finite element simulations indicate that damage could be detected and located when it occurred at mid-pan of an exterior girder. However, damage identification results from the experimental data indicate that damage cannot be consistently identified. This inability is caused by the fact that, in real-life bridge structures, environmental and operational effects may affect the vibration data the same way as damage. Therefore, it is suggested that future work be focused on minimizing the environmental and operational effects.
- This study is focused on damage identification of bridges in which damage is located on steel girders. It is suggested that for future work, damage which has occurred at abutment supports, bracing connections, and piers be considered.
- This study is mainly focused on developing time series-based damage identification so that the induced damage to two full-scale bridges can be detected and located. It is suggested that for future work, the analysis results be interpreted from the point of view

of bridge redundancy. The finite element models developed in this study will help the interpretation.

- This dissertation presents a limited study on multi-damage scenarios. It is suggested that for future work several damage locations be considered simultaneously under different loadings to see if the vibration-based damage identification techniques are still able to identify the damage.
- In real-life bridges, disasters usually occur under large loadings in which damage is propagated through the structure. It is suggested that future research consider a nonlinear model of a bridge to study progressive collapse under different loadings to see at which stage damage in a bridge structure is suitably identified, and then to estimate the remaining load capacity of the bridge.

Vita

Reza Vasheghani Farahani was born February 28, 1978 in Tehran, Iran. He received his Bachelor's degree in Civil Engineering from K.N. Toosi University of Technology in 2001. He earned his Master's degree in Civil Engineering from Amirkabir University of Technology (Tehran Polytechnic) in 2004. From 2004 to 2008 he worked as a senior structural engineer and deputy of Structural Department at the Moshanir Power Engineering Consultants. He later attended the University of Tennessee, Knoxville where he graduated with M.S. and Ph.D. degrees in Civil Engineering in Dec. 2010 and August 2013, respectively.